Science Translational Medicine AAAS

Submitted Manuscript: Confidential template updated: February 28 2012

Morphine causes itch through a distinct disinhibitory circuit

One Sentence Summary: This work shows that morphine-induced itch is mediated by a specific population of dynorphin-expressing spinal inhibitory neurons.

Authors: Eileen Nguyen[1,2], Grace Lim[3,4], Huiping Ding[5], Junichi Hachisuka[1], Mei-Chuan Ko[5], and Sarah E. Ross[1*]

Affiliations:

[1]University of Pittsburgh School of Medicine, Department of Neurobiology.

[2]University of Pittsburgh School of Medicine, Medical Scientist Training Program.

[3]University of Pittsburgh, Department of Anesthesiology & Perioperative Medicine.

[4]University of Pittsburgh, Department of Obstetrics, Gynecology, and Reproductive Sciences.

[5]Wake Forest School of Medicine, Department of Physiology and Pharmacology.

*Correspondence to: saross@pitt.edu.

Abstract: Morphine-induced itch is a very common and debilitating side effect that occurs in laboring women who receive epidural analgesia and in patients who receive spinal morphine for relief of perioperative pain. Although antihistamines are still widely prescribed for the treatment of morphine-induced itch, their use is controversial because the cellular basis for morphine-induced itch remains unclear. Here, we show that neuraxial morphine causes itch through neurons and not mast cells. In particular, we found that spinal dynorphin (Pdyn) neurons are both necessary and sufficient for morphine-induced itch. Notably, agonism of the kappa-opioid receptor alleviated morphine-induced itch in mice and non-human primates. Thus, our findings not only reveal that morphine causes itch through a mechanism of disinhibition but also challenge the long-standing use of antihistamines, thereby informing the treatment of millions worldwide.

Main text:

Introduction

Neuraxial morphine and other mu-opioid receptor agonists are routinely administered in hospitals around the world (*1*). For instance, many pregnant women undergoing labor receive epidural or spinal morphine (*2*–*4*). Moreover, epidural or spinal morphine is given as an analgesic for a large proportion of surgical procedures, including hip and knee arthroplasty (*5*).

Unfortunately, one of the major unwanted side effects of the spinal or epidural delivery routes is morphine-induced itch, which is observed in more than half of patients (*6–10*). First-generation antihistamines, such as diphenhydramine (the active ingredient in Benadryl), are commonly used in many hospitals globally to alleviate morphine-induced itch (*4*, *11*, *12*). The use of antihistamines likely stems from the observation that morphine causes histamine release from mast cells within the skin, and that histamine produces itch (*13–15*). Moreover, clinical data appear to support this idea because numerous studies confirm that antihistamines reduce itch in laboring women who receive morphine (*16–18*). However, though antihistamines are widely used to treat morphine-induced itch (*12*), whether this type of itch is indeed a result of peripheral histamine release has never been established and remains controversial (*19*, *20*).

To clarify how neuraxial morphine could cause itch, this study examines the contributions of both mast cells and inhibitory neurons on morphine-induced itch. We show that deletion of the mu-opioid receptor (Oprm1) from spinal dynorphin neurons eliminated neuraxial morphine-induced itch. Furthermore, we found that ectopic expression of the opioid receptor on dynorphin neurons was sufficient for itch. Lastly, we found that nalfurafine, a selective kappa-opioid receptor (Oprk1) agonist relieves morphine-induced itch without affecting analgesia in both mice and nonhuman primates, highlighting its potential clinical utility.

Results

Identification of endpoints for itch caused by morphine in mice and obstetric patients

Although it is clear that neuraxial morphine causes itch in humans (*6–10*), the characterization of clinical endpoints for morphine-induced itch remains limited. We found that morphine not only caused itch in women receiving spinal morphine for cesarean delivery, as previously reported (*9*, *10*), but also gave rise to clinical hyperknesis, as defined by exacerbation of itch in response to punctate stimulation (*21*), and clinical alloknesis, as defined by touch-evoked itch in response to brushing (*21*) (Fig. 1A and fig. S1A). These newly identified endpoints for morphine-induced itch in humans were highly correlated with overall self-reported itch ratings obtained using a numerical rating scale (fig. S1, B and C), suggesting that morphine-induced itch is accompanied by central sensitization (*21*). Next, we reverse-translated these findings in a mouse model (with even numbers of males and females) using an analgesic dose of morphine given intrathecally (300 pmol; I.T). In addition to morphine-induced scratching behavior, consistent with previous reports (*22*), mice showed morphine-induced hyperknesis, as demonstrated by an exacerbation of chloroquine-induced itch, as well as morphine-induced alloknesis, as revealed by touch-evoked itch in response to a von Frey filament (Fig. 1B and fig. S2, A to G). Thus, morphine-induced itch in mice appears to recapitulate our observations in humans, thereby enabling detailed mechanistic investigations of this phenomenon.

The roles of mast cells in morphine-induced itch

It is widely assumed that histamine release from degranulated mast cells in the skin underlies neuraxial morphine-induced itch (*9*). When given subcutaneously, morphine indeed causes degranulation of peripheral mast cells, which results in itch (*13–15*). However, the evidence for this mechanism is less clear for neuraxial morphine-induced itch; mast cells are not found in the spinal cord and emerging evidence has called the role of mast cells in neuraxial morphine-induced itch into question (*23*, *24*). Given the contested role of mast cells in morphine-

induced itch, we sought to determine their contribution to itch caused by either intrathecal (I.T.) or subcutaneous (S.C.) morphine (Fig. 2A). Consistent with previous results (*25*), we found that S.C. morphine caused site-directed scratching in mice in a dose-dependent manner (fig. S3A). In parallel experiments in which mice were given morphine but prevented from scratching, we observed that S.C. morphine (300 pmol) caused the degranulation of cutaneous mast cells that was similar in magnitude to that observed with the mast cell degranulator, compound 48/80 (Fig. 2B and fig. S3, B and C). In contrast, the same dose of I.T. morphine, although sufficient for robust analgesia (fig. S2, E to G), did not cause peripheral mast cell degranulation (Fig. 2B and fig. S3, B and C). Thus, neuraxial morphine for the purpose of analgesia is unlikely to cause the degranulation of mast cells in the periphery.

Diphenhydramine is clinically efficacious for neuraxial morphine-induced itch (*4*, *11*) and is frequently prescribed for its treatment (*4*). However, the site at which histamine receptor antagonists exert their effects to reduce itch remains unclear. To address this gap, we compared the effects of two antihistamine compounds in mice: diphenhydramine, a first-generation histamine receptor (H_1) antagonist that crosses the blood-brain barrier, and loratadine, a second-generation H_1 antagonist that remains peripherally restricted (Fig. 2A). As expected, both diphenhydramine and loratadine reduced itch caused by the degranulation of mast cells with compound 48/80 (fig. S3E). Similarly, scratching in response to S.C. morphine was reduced by both types of antihistamines (Fig. 2C), consistent with the idea that S.C. morphine causes itch that is mediated by peripheral histamine receptors (*25*). For I.T. morphine-induced itch, diphenhydramine was an effective treatment, just as is observed in humans (*4*) (Fig. 2D); in contrast, the peripherally restricted H_1 antagonist, loratadine, had no effect (Fig. 2D). Analogous findings were observed using I.T. gastrin releasing peptide (GRP) to cause central itch: only diphenhydramine reduced scratching bouts (fig. S3F). These findings suggest that H_1 antagonists must inhibit centrally-mediated itch through their action on a central target, but the mechanisms remained unclear. In this regard it is noteworthy that a concentration of diphenhydramine that reduced scratching behavior in mice was also accompanied by a reduction in their locomotor activity (Fig. 2, D and E and fig. S3, D to H). This locomotor effect is in keeping with the idea that drowsiness is a side effect of diphenhydramine in humans (*10*, *17*, *26*). Thus, although diphenhydramine reduces neuraxial-morphine induced scratching behavior, it is possible that this apparent reduction in itch may be secondary to somnolence (*27*).

To directly test whether mast cells are required for morphine-induced itch, we used a mouse model of mast cell depletion. Selective ablation of mast cells was achieved using $Mcpt5^{Cre}$ mice (*28*) together with Cre-dependent expression of diphtheria toxin ($Rosa^{DTA}$) (*29*) (Fig. 2F and fig. S3I). As expected, mice lacking mast cells no longer exhibited itch upon S.C. delivery of morphine (Fig. 2G). However, neuraxial morphine-induced itch was still intact in these mice (Fig. 2H). Overall, these findings indicate that mast cells are dispensable for neuraxial morphine-induced itch, and that, insofar as first-generation antihistamines reduce itch, this effect is central.

Pdyn neurons are required for neuraxial morphine-induced itch

Given that morphine-induced itch is most commonly seen in humans when morphine is given neuraxially (*10*), we next examined the possible role of spinal neurons. A previous study suggested that neuraxial morphine causes itch through activation of gastrin-releasing peptide receptor (Grpr) neurons in the dorsal horn (*19*), an excitatory population that is involved in mediating itch (*30*, *31*). However, when we performed dual fluorescent in-situ hybridization

(FISH) for *Oprm1* and *Grpr* in the dorsal horn, we found very limited overlap (fig. S4A). Because opioids typically signal through Gαi-coupled G-protein coupled receptors to inhibit neuronal activity (*32*, *33*), we favored the hypothesis that morphine causes itch through disinhibition. Therefore, we examined the expression of *Oprm1* across four distinct populations that account for the majority of inhibitory neurons in the dorsal horn (*34*): *Pdyn*, *Npy*, *Nos1*, and *Pvalb*. Through multiplex FISH, we found that roughly half of the neurons in the dorsal horn that express *Oprm1* are inhibitory neurons, as revealed by co-expression of *Slc32a1*, the gene encoding Vgat. Among these neurons, we found that *Oprm1* is expressed across all four populations, with the highest expression in Pdyn neurons (40.5±2.7% of Pdyn neurons express *Oprm1*, representing 33.0±1.0% of *Oprm1*-expressing inhibitory neurons in the dorsal horn) followed by Npy neurons (23.5±3.6% and 18.2±2.6%, respectively) (Fig. 3A and fig. S4, B and C).

The Pdyn and Npy inhibitory neurons were particularly intriguing to us because we and others had previously discovered that these two populations inhibit itch (*35*–*38*). Indeed, when either Pdyn neurons or Npy neurons are lost during development, mice show spontaneous scratching behavior suggesting that these populations are involved in the tonic inhibition of itch (*36*, *37*). We therefore investigated these populations in more detail, beginning with Pdyn neurons. Just as in rodents, we found that human *PDYN* neurons express *OPRM1*, as revealed by dual FISH of the spinal dorsal horn from post-mortem tissue (Fig. 3, A and B). Furthermore, recordings from tdTomato-labeled Pdyn neurons (in $Pdyn^{Cre}$; $Rosa^{tdt}$ mice) revealed that ~50% showed outward current in response to the Oprm1 agonist D-Ala^2, N-$MePhe^4$, Gly-ol-enkephalin (DAMGO) (Fig. 3C), consistent with the idea that Pdyn cells express functional Oprm1 and that activation of this receptor inhibits the cells.

Based on these findings, we next asked whether expression of *Oprm1* in Pdyn neurons was required for morphine-induced itch. Using a conditional deletion strategy, we selectively removed *Oprm1* from Pdyn neurons (Fig. 3D). Strikingly, this genetic manipulation completely eliminated I.T. morphine-induced itch, hyperknesis, and alloknesis (Fig. 3, E to G). Importantly, morphine-induced increases in paw withdrawal latency was unaffected in these animals (Fig. 3H), indicating that Oprm1 expression on Pdyn neurons is required for morphine-induced itch but not morphine-induced analgesia. Because our data suggested that Npy neurons also express *Oprm1* (Fig. 3A and fig. S4C) and because these cells are known to inhibit itch, we next examined the contribution of this population. In contrast to Pdyn neurons, conditional deletion of *Oprm1* from Npy neurons had no effect on neuraxial morphine-induced itch (Fig. 3I and fig. S5, A to D). These findings identify Pdyn neurons as the cellular mediator of morphine-induced itch.

Inhibition of Pdyn neurons elicits itch

Our loss-of-function experiments implied that morphine causes itch through disinhibition of Pdyn cells. To test this idea directly, we sought to mimic opioid signaling in these cells through chemogenetic manipulation using either KORD or hM4Di, two Gi-coupled designer receptors exclusively activated by designer drugs (DREADDs). In these experiments, we injected Cre-dependent adeno-associated viruses (AAVs) into the lumbar spinal cord of $Pdyn^{Cre}$ mice (Fig. 4A and fig. S6, A to D). Notably, in both approaches, chemogenetic inhibition of Pdyn neurons elicited spontaneous itch in the form of increased time spent biting the leg (the dermatome segment that corresponded to the site of viral delivery) (Fig. 4, B and C). We also observed hyperknesis and alloknesis, but no changes to heat sensitivity, upon chemogenetic

inhibition of Pdyn neurons (Fig. 4, D to F). Together, these findings suggest that morphine causes itch through inhibition of Pdyn neurons, resulting in disinhibition.

Activation of kappa opioid receptor signaling alleviates morphine-induced itch in mice and non-human primates

Next, studies involving the immediate-early gene *Fos* were performed to examine the mechanism through which the inhibition of Pdyn neurons by morphine causes itch (Fig. 5A). Following I.T. morphine, we found an upregulation of *Fos* expression in neurons that express the kappa opioid receptor (Oprk1), consistent with the idea that inhibition of Pdyn neurons results in disinhibition (activation) of Oprk1 neurons (Fig. 5, B and C, and fig. S7A). Because Pdyn neurons release several inhibitory mediators, including dynorphin and GABA (*39*, *40*), we wondered which ones might be involved (Fig. 5A). Therefore, we performed occlusion studies using the long-acting Oprk1 antagonist nor-binaltorphimine dihydrochloride (norBNI) to inhibit Oprk1 (fig. S8, A and B). Significant scratching was observed in mice pretreated with I.T. norBNI (fig. S8A), consistent with the idea that ongoing dynorphin tone in the spinal cord inhibits itch, as previously described (*38*). However, pretreatment with norBNI did not prevent morphine from causing further itch (fig. S8A). This lack of occlusion suggests that morphine-induced itch is not due solely to the inhibition of dynorphin release, and might therefore involve the disinhibition of Oprk1 neurons through a reduction in both dynorphin and GABA activity.

Our model suggested that inhibition of Oprk1 neurons should alleviate morphine-induced itch. To test this idea, we examined the effect of nalfurafine, a selective Oprk1 agonist (*41*). In mice, we found that co-administration of nalfurafine and morphine (I.T.) reduced morphine-induced itch, hyperknesis, and alloknesis compared to controls (Fig. 5, D to F and fig. S7, B to D). Importantly, the dose of nalfurafine that abrogated morphine-induced itch did not reduce the analgesic efficacy of morphine to thermal sensitivity (Fig. 5G and fig. S7E). These findings suggest that inhibition of Oprk1 neurons suppresses morphine-induced itch without reducing morphine's analgesic effects.

To examine the translational relevance of these findings, we repeated these experiments in non-human primates. Again, I.T. nalfurafine reduced the number of morphine-induced scratches without affecting analgesia to tail withdrawal (Fig. 6, A and B, and fig. S7, F and G). Thus, in both mouse as well as non-human primate models, we observed that treatment with an Oprk1 agonist mitigates morphine-induced itch without affecting morphine-induced analgesia.

Discussion

In this study, we first addressed the long-standing controversy regarding the mechanism through which antihistamines block neuraxial morphine-induced itch by demonstrating that mast cells are not involved. Instead, our studies suggest that the apparent reduction in itch mediated by centrally-acting antihistamines may be secondary to their somnolescent effects. Next, we discovered that Oprm1 expression in Pdyn neurons is required for neuraxial morphine-induced itch and that chemogenetic inhibition of Pdyn neurons is sufficient to cause itch. Lastly, we activated Oprk1 signaling using nalfurafine, an Oprk1 agonist, to block morphine-induced itch in mice and non-human primates. Together, these findings reveal a distinct disinhibitory neural circuit for morphine-induced itch, which has important implications for the clinical management of this condition.

Diphenhydramine is still frequently prescribed as a first-line treatment for morphine-induced itch (*7*, *9*). However, clinicians have observed that the sedating effects of antihistamines have caused patients to verbally deny itch while continuing to scratch, and that patients are itchy in between periods of sleep (*10*, *17*, *26*). Histaminergic neurons in the tuberomammillary nucleus of the posterior hypothalamus are thought to promote wakefulness through their activation of H_1R, and antihistamines are thought to cause sedation through the antagonism of these receptors, which are widely distributed in the brainstem (*42*) and cortex (*43–45*). Importantly, this unwanted side effect of sedation is particularly undesirable in the context of morphine-induced itch because it raises safety concerns due to the potential of antihistamines to exacerbate respiratory depression caused by opioids (*7*, *26*, *46*).

Our results challenge the practice of using diphenhydramine for neuraxial morphine-induced itch because we show that mast cells are not involved. In addition, the finding that diphenhydramine only reduces scratching at a dose that also suppresses locomotor activity (Fig. 2E) further underscores the concept that the use of antihistamines for neuraxial morphine-induced itch may be inappropriate.

In human, non-human primate, and mouse models, we have validated that neuraxial morphine causes itch (*6–10*, *19*, *22*, *24*, *47*, *48*). Intriguingly, although neuraxial morphine elicited itch in all three species, the duration of itch in humans and non-human primates was longer than that observed in mice. This difference in duration of morphine action likely reflects species differences in a variety of factors that influence drug distribution and half-life, including the relative expression levels of metabolic enzymes, receptor signaling, and trafficking (*49*). Nevertheless, the finding that nalfurafine reduces morphine-induced itch in both mice and non-human primates suggests a common underlying circuit mechanism, which we have revealed in our study.

It was previously suggested that an excitatory population of Grpr spinal neurons mediates morphine-induced itch through a specific isoform of the mu-opioid receptor, *MOR1D* (*19*). However, we observed very little overlap in the dorsal horn between *Grpr* and *Oprm1* using a probe that targets a region common to all *Oprm1* isoforms, including *MOR1D* (fig. S4A). Although several studies have implicated differential contributions of *Oprm1* isoforms in opioid-induced pruritus and analgesia (*50–52*), the specific isoform in Pdyn neurons that is responsible for morphine-induced itch was not addressed in the current study because the genetic strategy used here does not distinguish among splice variants.

Our study has uncovered a previously undescribed role for neuronal disinhibition in morphine-induced itch and highlights the idea that distinct opioids (e.g., mu and kappa) differentially modulate somatosensation. We find that mu-opioid signaling inhibits dynorphin neurons and although we do not yet know the degree to which this modulation involves dynorphin or GABA release from these cells, our occlusion studies raise the possibility that both may be involved. In any case, the finding that nalfurafine reverses morphine-induced itch suggests that Oprk1 neurons are the relevant target for inhibition by Pdyn neurons. Our studies also suggest that nalbuphine (a mixed kappa agonist and mu antagonist that is frequently prescribed in the setting of opioid-induced pruritus) (*7*, *9*) likely works to inhibit morphine-induced itch, at least in part, by virtue of its ability to activate Oprk1. However, a major limitation of nalbuphine is that it reduces the analgesia provided by morphine (*7*, *46*). Unlike nalbuphine, nalfurafine does not affect the therapeutic analgesia provided by morphine (Fig. 5G and Fig. 6B). Thus, our results not only provide a mechanistic explanation for how nalbuphine

reduces morphine-induced itch, but also reveal a circuit mechanism through which a selective Oprk1 agonist, such as nalfurafine, can be used for the treatment of clinical neuraxial morphine-induced itch in humans.

Materials and Methods

Study design

The objective of the study was to determine the cellular basis for neuraxial morphine-induced itch. To achieve this, we examined the contribution of spinal dynorphin neurons to neuraxial morphine-induced itch. We used intersectional mouse genetics to selectively determine whether dynorphin neurons are necessary and sufficient for morphine-induced itch. To test translatability of our findings in mice, we recruited a cohort of human participants receiving spinal morphine to assess morphine-induced itch. Finally, we also tested a pharmacological treatment for morphine-induced itch and mice and non-human primates. Animals were randomly assigned to control and treatment groups. Data was acquired and analyzed in a blinded manner. Biological replicates were obtained for each experiment (specific values are provided in the figure legends).

Human subjects

A prospective observational approach was chosen. Written, informed consent was obtained from all research participants and this study was approved by the University of Pittsburgh Institutional Review Board (Study #19050109). A convenience sampling of women aged 18 years or older with scheduled cesarean sections was conducted. Exclusion criteria included chronic pain, current opioid maintenance therapy, or emergency cesarean delivery. Upon enrollment, morphine-induced itch, hyperknesis, and alloknesis were established, each using a numerical rating scale (NRS) (e.g., "How itchy do you currently feel?"). Zero indicated "no intensity (or unpleasantness) at all" and 10 indicated "the most intense (or unpleasant) itch I can imagine." Hyperknesis was assessed using a 2.0 gram von Frey monofilament applied to a distal extremity. Alloknesis was assessed using a brush (SenseLab, Somedic AB, Sweden) applied to a distal extremity. Assessments occurred during hospitalization prior to and 24 hours after cesarean delivery. Responses were de-identified, coded, and stored on a secure, web-based application on Research Electronic Data Capture (REDCap).

Mice

The studies were performed in both male and female mice 8-10 weeks of age. All animals were of the C57/Bl6 background. Even numbers of male and female mice were used for all experiments. No sex differences were found and, thus, animals were pooled. Mice were given food and water ad libitum and housed under standard laboratory conditions. $Pdyn^{Cre}$, Npy^{Cre}, $Oprm1^{fl/fl}$, $Mcpt5^{Cre}$, $Rosa^{DTA}$, and Ai34(RCL-Syp/tdT)-D ($Rosa^{tdt}$) back-crossed into the C57/Bl6 background were bred and raised at the University of Pittsburgh. $Pdyn^{Cre}$ (Jax #027958), Npy^{Cre} (Jax #027851), $Oprm1^{fl/fl}$ (Jax #030074), $Rosa^{DTA}$ (Jax #009669), and $Rosa^{tdt}$ (Jax #012570) mice are available at Jackson Laboratories. $Mcpt5^{Cre}$ mice were a gift from Axel Roers (Dresden University of Technology). The use of animals was approved by the Institutional Animal Care and Use Committee of the University of Pittsburgh.

Non-human primates

All animal care and experiments in non-human primate study were conducted according to the Guide for the Care and Use of Laboratory Animals by the US National Institutes of Health (Bethesda, MD, USA), reported according to the ARRIVE guidelines (*53*), and approved by the Institutional Animal Care and Use Committee of Wake Forest University (Winston-Salem, NC, USA). Five adult male and female rhesus monkeys (Macaca mulatta), 8–16 years of age, 5.1–12.2 kg, with implanted intrathecal catheters (*54*) were used in this study. The monkeys were

housed at an indoor facility accredited by the Association for Assessment and Accreditation of Laboratory Animal Care International (Frederick, MD, USA). The monkeys were individually housed in cages with 6-12 square feet of floor space with ceilings 2.7-5.4 feet high in a temperature controlled room (21–25 °C, 40–60% relative humidity) with a 12-h light/dark cycle (Light On: 6:30-18:30). The monkeys were provided with water and their diet consisted of approximately 20–30 biscuits (Purina Monkey Chow; Ralston Purina Co., St. Louis, MO, USA) and fresh fruit ad libitum. Primate enrichment devices and small amounts of treats were provided daily.

Drug administration in non-human primates

Morphine sulfate (National Institute on Drug Abuse, Bethesda, MD, USA) and nalfurafine HCl (provided by Dr. Stephen Husbands, University of Bath, Bath, UK) were dissolved in sterile water. For intrathecal administration (*54*), 1 mL of the test compound was administered through the subcutaneous access port, followed by 0.35 mL of saline to flush the dead volume of the port and catheter.

Pharmacologic agents used in mice

Morphine sulfate (4 mg/ml; Henry Schein Animal Health) and chloroquine diphosphate salt (Sigma) were dissolved in physiological saline. Salvinorin B (SalB; Tocris) was dissolved in DMSO and administered subcutaneously (10 mg/kg). Clozapine-N-oxide (CNO; Tocris) was dissolved in PBS and administered intraperitoneally (5mg/kg). nor-Binaltorphimine dihydrochloride (norBNI; Sigma) was administered as previously described (*38*). Mice were pretreated with norBNI (1 μg in 5 μL) 24 hours prior to experimentation. Nalfurafine (Sigma) was dissolved in saline and administered intrathecally. Loratadine (Sigma) and diphenhydramine (Sigma) were prepared in 10% DMSO and given 10 mg/kg I.P. For experiments involving antihistamines, animals were pretreated with vehicle, loratadine, or diphenhydramine 30 minutes prior to recording scratching behavior.

Intradermal and intrathecal injections

For intradermal injection of chloroquine, hair was clipped from the neck or calf of each mouse at least 24 hours before the experiment. Chloroquine (100 μg in 10 μL) was administered into the nape of the neck or calf, which could be subsequently visualized by the formation of a small bubble under the skin. For intrathecal injections, hair was clipped from the back of each mouse at least 24 hours before the experiment. All intrathecal injections were delivered in a total volume of 5 μL using a 30-gauge needle attached to a luer-tip 25 μL Hamilton syringe. The needle was inserted into the tissue at a 45° angle through the fifth intervertebral space (L5 – L6). Solution was injected at a rate of 1 μL/s. The needle was held in position for 10 seconds and removed slowly to avoid any outflow of the solution. Only mice that exhibited a reflexive flick of the tail following puncture of the dura were included in behavioral analysis. These procedures were performed in awake, restrained mice.

Intraspinal injections

Mice were anesthetized with 100 mg/kg ketamine and 10 mg/kg xylazine. An incision was made at the spinal cord level corresponding to L4-6 dermatome. The intrathecal space was exposed, and two injections of approximately 300 nl of virus (AAV8-DF-KORD-mCitrine, Addgene #65417; AAV2.hSyn.DIO.mCherry Addgene #50459; AAV2.hSyn.DIO.hM4D(Gi)-mCherry, Addgene #44362) were infused 300 mm below the surface of the spinal cord at 5 nL/s via glass

pipette through the intrathecal space corresponding to L4-6 of the spinal cord. The glass pipette was left in place for an additional 5 minutes before withdrawal. The incision was closed with 5-0 vicryl suture. Ketofen was delivered I.P. 10 mg/kg and mice were allowed to recover over a heat pad. The injections were validated post-mortem by fluorescent in-situ hybridization of *Pdyn* and *eYFP* or *mCherry* to detect KORD-mCitrine or hM4Di-mCherry, respectively.

All behavioral tests described below were performed in a blinded manner.

Observation of scratching behavior

Scratching behavior was observed using a previously reported method (*38*). Mice were individually placed in the observation cage (12 x 9 x 14 cm) to acclimate for 30 minutes. The mice were assigned to dosing conditions in a randomized manner. For dose-dependent subcutaneous morphine-induced itch, animals received either 5 μL morphine (0.3, 3, or 300 pmol) or saline to the nape of the neck. Scratching behavior was videotaped for 60 minutes after administration. For all other experiments, unless otherwise indicated, 300 pmol of morphine was administered (S.C. and I.T.). The total numbers of scratch bouts by the hind paws at various body sites during the first 60 minutes after subcutaneous (morphine or 48/80) intrathecal injection (morphine or 100 pmol GRP) were counted. For subcutaneous injections, only scratch bouts directed to the nape of the neck were counted. For experiments directed at the calf, the amount of time spent biting the leg was quantified over 60 minutes. Both control and KORD or control and hM4Di treated animals were pretreated with SalB or CNO, respectively, 30 minutes prior to the start of the experiment.

To assess the effect of nalfurafine on intrathecal morphine-induced itch in non-human primates, scratching activity (*20*) was recorded when monkeys were in their home cages. Each 15-minute recording session was conducted at 0.5, 1, 2, 2.5 and 3 hours following intrathecal morphine administration. Nalfurafine (0.1 or 0.3 μg) or vehicle was intrathecally administered at 1.5 hours after intrathecal morphine (10 or 30 μg) administration. A scratch was defined as one brief (<1 second) action of scraping on the skin surface of other body parts using the forepaw or hind paw (*20*). The total number of scratches were counted and summed for each 15-minute period.

Acute thermal nociception

To assess the effect of nalfurafine on intrathecal morphine-induced antinociception in non-human primates, nalfurafine (0.3 μg) or vehicle was intrathecally administered at 1.5 hours after intrathecal morphine (10 μg). The warm water tail-withdrawal assay (*55*) was conducted before and 0.5, 1, 2, 2.5 and 3 hours after intrathecal morphine administration. The lower parts of their shaved tails (~15 cm) were immersed in water maintained at 42, 46, or 50 °C. The monkeys were assigned to dosing conditions in a randomized manner. Water at 42 or 46 °C was used as a non-noxious stimuli (i.e., no tail-withdrawal movement was expected), and water at 50 °C was used as an acute noxious stimulus (i.e., 2-3 second tail-withdrawal latency). Experimenters measured tail-withdrawal latencies at each temperature by using a computerised timer. If a monkey did not withdraw its tail within 20 seconds (cut-off), the stimulus was removed and a maximum time of 20 seconds was recorded.

Heat sensitivity assay (Hargreaves testing)

Mice were acclimated on a glass plate held at 30°C (IITC Life Science Inc.). A radiant heat source (activity intensity of 15%) was applied to the hindpaw and latency to paw withdrawal was

recorded (*56*). Two trials were conducted on each paw, with at least 5 minutes between testing the opposite paw and at least 10 minutes between testing the same paw. To avoid tissue damage, a cut off latency of 20 seconds was set. Values from both paws were averaged to determine withdrawal latency.

Alloknesis

One hour after the intrathecal injection of morphine, mice were assessed for alloknesis. As previously described (*57*), alloknesis was assessed by delivering 3 separate innocuous mechanical stimuli using a von Frey filament (bending force: 0.7 mN; Stoetling, USA) every 5 minutes. Each application of the von Frey filament was reported as 1 trial, yielding a total of 18 trials over 30 minutes.

Hyperknesis

One hour after the intrathecal injection of morphine, mice were assessed for hyperknesis. Chloroquine (100 μg in 10 μL) was injected intradermally into the nape of the neck or calf and scratching behavior was recorded for 30 minutes. The total number of scratch bouts by the hand paws directed to the nape of the neck was counted. For hyperknesis following chemogenetic inhibition, chloroquine (100 μg in 10 μL) was injected intradermally into the calf and biting behavior was recorded for 30 minutes.

Open field activity

Spontaneous activity in the open field was conducted over 30 minutes in an automated Versamax Legacy open field apparatus for mice (Omnitech Electronics Incorporated, Columbus, OH). Distance traveled (s), ambulatory average velocity (cm/s), and ambulatory time (s) were measured by infrared photobeams located around the perimeter of the arenas interfaced to a computer running Fusion v.6 for Versamax software (Omnitech Electronics Incorporated) which monitored the location and activity of the mouse during testing. Activity plots were generated using the Fusion Locomotor Activity Plotter analyses module (Omnitech Electronics Incorporated). To determine whether antihistamines would modify locomotion, mice were placed into the open field 30 post vehicle, loratadine, or diphenhydramine treatment. For all tests, mice were transferred to the testing room one hour prior to testing.

Human Tissue Samples

Human spinal cord fresh-frozen tissues were obtained from the NeuroBioBank, National Institutes of Health (Project # 063772) and provided by Dr. Jill Glausier, Department of Psychiatry, University of Pittsburgh. All available evidence indicated these subjects did not have any major psychiatric illness, nor any neuropathological illness, at the time of death. All procedures were approved by the Committee for the Oversight of Research and Clinical Training Involving Decedents at the University of Pittsburgh, Pittsburgh, Pennsylvania.

RNAscope fluorescent in-situ hybridization

Multiplex fluorescent in-situ hybridization (FISH) was performed according to the manufacturer's instructions (Advanced Cell Diagnostics #320850). Briefly, 16 μm-thick fresh-frozen sections containing the mouse or human spinal cord were fixed in 4% paraformaldehyde, dehydrated, treated with protease for 15 minutes, and hybridized with gene- and species-specific probes. Probes were used to detect Mm-eYFP-C1 (#312131), Mm-mCherry-C2 (#431201), Mm-Oprm1-C1 (#315841), Mm-Oprk1-C1 (#316111), Mm-Npy-C2 (#313321-C2), Mm-Pdyn-C2

(#318771-C2), Mm-GRPR-C2 (#317871-C2), Mm-Pvalb-C2 (#421931-C2), Mm-Nos1-C2 (#437651-C2), Mm-Fos-C3 (#498401-C3), Mm-Slc31a1-C3 (#319191), Mm-Slc17a6-C3 (#319171), Hs-OPRM1-C1 (#410681), Hs-PDYN-C2 (#507161-C2). DAPI (#320858) was used to visualize nuclei. 3-plex positive (#320881) and negative (#320871) control probes were tested.

Immunohistochemistry

Mice were anesthetized with an intraperitoneal injection of urethane, transcardially perfused, and post-fixed at least four hours in 4% paraformaldehyde. 25 μm thick spinal cord or dorsal root ganglion sections were collected on a cryostat and slide-mounted for immunohistochemistry. Sections were blocked at room temperature for two hours in a 5% donkey serum, 0.2% triton, in phosphate buffered saline. Primary antisera was incubated for 14 hours overnight at 4°C with rabbit anti-RFP (1:1K; Cat #600-401-379, Rockland, USA). Sections were subsequently washed and incubated in secondary antibodies (Life Technologies, 1:500) at room temperature for two hours. Sections were then incubated in Hoechst (ThermoFisher, 1:10K) for 1 minute and washed, mounted, and a cover slip was applied.

Image acquisition and quantification

Full-tissue thickness sections were imaged using either an Olympus BX53 fluorescent microscope with UPlanSApo 4x, 10x, or 20x objectives or a Nikon A1R confocal microscope with 20X or 60X objectives. All images were quantified and analyzed using ImageJ. To quantify images in RNAscope in-situ hybridization experiments, confocal images of tissue samples (3-4 dorsal horns per mouse over 3-4 mice or 5-6 images per dorsal horn from two human spinal cords) were imaged and only cells whose nuclei were clearly visible by DAPI staining and exhibited fluorescent signal were counted.

Quantification of mast cells

For staining of cutaneous mast cells, hair was removed from the nape of the neck two days prior to S.C. injection. S.C. injections for histological analyses were performed in lightly anesthetized (isoflurane) animals to prevent the confounds of scratching on degranulation. Skin and dural samples were collected fresh-frozen, sectioned at 8 μm, and post-fixed in 4% PFA for 60 minutes. Toluidine blue was used to stain mast cells. Images were collected using a TissueGnostics brightfield microscope. Compound 48/80 (100 μg, Sigma) was used as a positive control for mast cell degranulation. Mast cells that contained a nucleus surrounded by granules were considered to be degranulated.

Quantification of *Fos*

Mice were lightly anesthetized with isoflurane before receiving I.T. morphine or saline. Twenty minutes later, their spinal cords were harvested for FISH. The total number of cells co-expressing *Fos, Oprk1,* and *Slc17a6* were counted and compared to the total number of cells co-expressing *Oprk1* and *Slc17a6*.

Electrophysiological recordings

The semi-intact somatosensory preparation was made as previously described (*58*, *59*). Briefly, young adult mice (5–9 weeks old) were deeply anesthetized and perfused transcardially through the left ventricle with oxygenated (95% O2 and 5% CO2) sucrose-based artificial cerebrospinal fluid (ACSF) (in mM; 234 sucrose, 2.5 KCl, 0.5 CaCl2, 10 MgSO4, 1.25 NaH2PO4, 26 NaHCO3, 11 Glucose) at room temperature. Immediately following perfusion, the skin was

incised along the dorsal midline and the spinal cord was quickly exposed via dorsal laminectomy. The right hindlimb and spinal cord (~C2 – S6) were excised, transferred into Sylgard-lined dissection/recording dish, and submerged in the same sucrose-based ACSF, which circulated at 50 ml/min to facilitate superfusion of the cord. The skin innervated by the saphenous nerve and the femoral cutaneous nerve was dissected free of surrounding tissue. L2 and L3 DRG were left on the spine. Pial membrane was carefully removed and the spinal cord was pinned onto the Sylgard chamber with the right dorsal horn facing upward. Following dissection, the chamber was transferred to the rig. Then the preparation was perfused with normal ACSF solution (in mM; 117 NaCl, 3.6 KCl, 2.5 $CaCl_2$, 1.2 $MgCl_2$, 1.2 NaH_2PO_4, 25 $NaHCO_3$, 11 glucose) saturated with 95% O_2 and 5% CO_2 at 32 °C. Tissue was rinsed with ACSF for at least 30 min to wash out sucrose. Thereafter, recordings were performed for up to 6 hours post-dissection.

Patch clamp recording from dorsal horn neurons

Neurons were visualized using a fixed stage upright microscope (BX51WI Olympus microscope, Tokyo, Japan) equipped with a 40x water immersion objective lens, a CCD camera (ORCA-ER Hamamatsu Photonics, Hamamatsu City, Japan) and monitor screen. A narrow beam infrared LED (L850D-06 Marubeni, Tokyo, Japan, emission peak, 850 nm) was positioned outside the solution meniscus, as previously described (*58*, *60*, *61*). $Pdyn^{Cre}$ neurons in lamina I were easily identified by td-Tomato expression. Whole-cell patch-clamp recordings were made with a pipette constructed from thin-walled single-filamented borosilicate glass using a microelectrode puller (PC-10; Narishige International, East Meadow NY). Pipette resistances ranged from 6 to 12 MΩ. Electrodes were filled with an intracellular solution containing the following (in mM): 135 K-gluconate, 5 KCl, 0.5 $CaCl_2$, 5 EGTA, 5 HEPES, 5 MgATP, pH 7.2. Alexa fluor 488 (Invitrogen; 25 µM) was added to confirm recording from the target cell. Signals were acquired with an amplifier (Axopatch 200B, Molecular Devices, Sunnyvale CA). The data were low-pass filtered at 2 kHz and digitized at 10 kHz with an A/D converter (Digidata 1322A, Molecular Devices) and stored using a data acquisition program (Clampex version 10, Molecular Devices). The liquid junction potential was not corrected.

Statistical analysis

All statistical analyses were performed using GraphPad Prism 7. Values are presented as mean ± SEM. *P* values were determined by tests indicated in applicable figure legends. Sample sizes were based on pilot data and are similar to those typically used in the field.

Supplementary Materials:

Fig. S1. Morphine-induced itch, hyperknesis, and alloknesis in obstetric patients.

Fig. S2. Morphine-induced itch, hyperknesis, and alloknesis in mice.

Fig. S3. Differential role of mast cells on subcutaneous vs. intrathecal morphine-induced itch.

Fig. S4. Spinal expression of *Oprm1* in *Grpr*, *Pdyn*, and *Npy* neurons.

Fig. S5. Expression of *Oprm1* in *Npy* neurons is not required for morphine-induced itch

Fig. S6. Validation of viral infection of Pdyn neurons.

Fig. S7. Dose-response analysis of nalfurafine treatment for morphine-induced itch.

Fig. S8. Antagonism of the kappa-opioid receptor evokes itch.

Data File S1. Individual-level data in tabular format.

References:

1. B. Waxler, Z. P. Dadabhoy, L. Stojiljkovic, S. F. Rabito, Primer of Postoperative Pruritus for Anesthesiologists. *Anesthesiology: The Journal of the American Society of Anesthesiologists* (2005).

2. A. J. Butwick, C. A. Wong, N. Guo, Maternal Body Mass Index and Use of Labor Neuraxial Analgesia: A Population-based Retrospective Cohort Study. *Anesthesiology*. **129**, 448–458 (2018).

3. S. Alran, O. Sibony, J.-F. Oury, D. Luton, P. Blot, Differences in management and results in term-delivery in nine European referral hospitals: descriptive study. *Eur. J. Obstet. Gynecol. Reprod. Biol.* **103**, 4–13 (2002).

4. K. Kumar, S. I. Singh, Neuraxial opioid-induced pruritus: An update. *J. Anaesthesiol. Clin. Pharmacol.* **29**, 303–307 (2013).

5. A. D. Kaye *et al.*, Enhanced recovery pathways in orthopedic surgery. *J. Anaesthesiol. Clin. Pharmacol.* **35**, S35–S39 (2019).

6. B. Waxler, Z. P. Dadabhoy, L. Stojiljkovic, S. F. Rabito, Primer of postoperative pruritus for anesthesiologists. *Anesthesiology*. **103**, 168–178 (2005).

7. R. G. Jannuzzi, Nalbuphine for Treatment of Opioid-induced Pruritus: A Systematic Review of Literature. *Clin. J. Pain*. **32**, 87–93 (2016).

8. A. Ganesh, L. G. Maxwell, Pathophysiology and management of opioid-induced pruritus. *Drugs*. **67**, 2323–2333 (2007).

9. S. Szarvas, D. Harmon, D. Murphy, Neuraxial opioid-induced pruritus: a review. *J. Clin. Anesth.* **15**, 234–239 (2003).

10. J. C. Ballantyne, A. B. Loach, D. B. Carr, Itching after epidural and spinal opiates. *Pain*. **33**, 149–160 (1988).

11. S. M. Siddik-Sayyid *et al.*, Ondansetron is as effective as diphenhydramine for treatment of morphine-induced pruritus after cesarean delivery. *Acta Anaesthesiol. Scand.* **54**, 764–769 (2010).

12. G. W. M. Millington *et al.*, British Association of Dermatologists' guidelines for the investigation and management of generalized pruritus in adults without an underlying dermatosis, 2018. *Br. J. Dermatol.* **178**, 34–60 (2018).

13. K. Lansu *et al.*, In silico design of novel probes for the atypical opioid receptor MRGPRX2. *Nat. Chem. Biol.* **13**, 529–536 (2017).

14. N. Grosman, Histamine release from isolated rat mast cells: effect of morphine and related drugs and their interaction with compound 48/80. *Agents Actions*. **11**, 196–203 (1981).

15. J. M. Hermens, J. M. Ebertz, J. M. Hanifin, C. A. Hirshman, Comparison of histamine release in human skin mast cells induced by morphine, fentanyl, and oxymorphone. *Anesthesiology*. **62**, 124–129 (1985).

16. C.-C. Liao *et al.*, Efficacy of intramuscular nalbuphine versus diphenhydramine for the prevention of epidural morphine-induced pruritus after cesarean delivery. *Chang Gung Med. J.* **34**, 172–178 (2011).

17. M. L. Horta *et al.*, Study of the prophylactic effect of droperidol, alizapride, propofol and promethazine on spinal morphine-induced pruritus. *Br. J. Anaesth.* **96**, 796–800 (2006).

18. J. Eldor, V. Fishelev, S. Levine, P. Guedj, I. Dudakova, Prevention of epidural morphine pruritus by intramuscular promethazine in parturients. *Reg. Anesth.* **19**, 433–434 (1994).

19. X.-Y. Liu *et al.*, Unidirectional cross-activation of GRPR by MOR1D uncouples itch and analgesia induced by opioids. *Cell*. **147**, 447–458 (2011).

20. M. C. H. Ko, M. S. Song, T. Edwards, H. Lee, N. N. Naughton, The role of central mu opioid receptors in opioid-induced itch in primates. *J. Pharmacol. Exp. Ther.* **310**, 169–176 (2004).

21. H. H. Andersen *et al.*, Alloknesis and hyperknesis-mechanisms, assessment methodology, and clinical implications of itch sensitization. *Pain*. **159**, 1185–1197 (2018).

22. M. Sakakihara, N. Imamachi, Y. Saito, Effects of Intrathecal κ-Opioid Receptor Agonist on Morphine-Induced Itch and Antinociception in Mice. *Reg. Anesth. Pain Med.* **41**, 69–74 (2016).

23. L. Edvinsson, J. Cervós-Navarro, L. I. Larsson, C. Owman, A. L. Rönnberg, Regional distribution of mast cells containing histamine, dopamine, or 5-hydroxytryptamine in the mammalian brain. *Neurology*. **27**, 878–883 (1977).

24. M.-C. Ko, Neuraxial opioid-induced itch and its pharmacological antagonism. *Handb. Exp. Pharmacol.* **226**, 315–335 (2015).

25. H. Melo *et al.*, Itch induced by peripheral mu opioid receptors is dependent on TRPV1-expressing neurons and alleviated by channel activation. *Sci. Rep.* **8**, 15551 (2018).

26. T. Roth, T. Roehrs, G. Koshorek, J. Sicklesteel, F. Zorick, Sedative effects of antihistamines. *J. Allergy Clin. Immunol.* **80**, 94–98 (1987).

27. J. Kamei, S. Hirano, S. Miyata, A. Saitoh, K. Onodera, Effects of first- and second-generation histamine-H1-receptor antagonists on the pentobarbital-induced loss of the righting reflex in streptozotocin-induced diabetic mice. *J. Pharmacol. Sci.* **97**, 266–272 (2005).

28. J. Scholten *et al.*, Mast cell-specific Cre/loxP-mediated recombination in vivo. *Transgenic Res.* **17**, 307–315 (2008).

29. N. Schubert *et al.*, Unimpaired Responses to Vaccination With Protein Antigen Plus Adjuvant in Mice With Kit-Independent Mast Cell Deficiency. *Front. Immunol.* **9**, 1870 (2018).

30. Y.-G. Sun, Z.-F. Chen, A gastrin-releasing peptide receptor mediates the itch sensation in the spinal cord. *Nature*. **448**, 700–703 (2007).

31. M. Pagani *et al.*, How Gastrin-Releasing Peptide Opens the Spinal Gate for Itch. *Neuron*. **103**, 102-117.e5 (2019).

32. R. Al-Hasani, M. R. Bruchas, Molecular mechanisms of opioid receptor-dependent signaling and behavior. *Anesthesiology*. **115**, 1363–1381 (2011).

33. M. Torrecilla, N. Quillinan, J. T. Williams, K. Wickman, Pre- and postsynaptic regulation of locus coeruleus neurons after chronic morphine treatment: a study of GIRK-knockout mice. *Eur. J. Neurosci.* **28**, 618–624 (2008).

34. K. A. Boyle *et al.*, A quantitative study of neurochemically defined populations of inhibitory interneurons in the superficial dorsal horn of the mouse spinal cord. *Neuroscience*. **363**, 120–133 (2017).

35. D. Acton *et al.*, Spinal Neuropeptide Y1 Receptor-Expressing Neurons Form an Essential Excitatory Pathway for Mechanical Itch. *Cell Rep.* **28**, 625-639.e6 (2019).

36. S. Bourane *et al.*, Gate control of mechanical itch by a subpopulation of spinal cord interneurons. *Science*. **350**, 550–554 (2015).

37. S. E. Ross *et al.*, Loss of inhibitory interneurons in the dorsal spinal cord and elevated itch in Bhlhb5 mutant mice. *Neuron*. **65**, 886–898 (2010).

38. A. P. Kardon *et al.*, Dynorphin acts as a neuromodulator to inhibit itch in the dorsal horn of the spinal cord. *Neuron*. **82**, 573–586 (2014).

39. T. C. P. Sardella *et al.*, Dynorphin is expressed primarily by GABAergic neurons that contain galanin in the rat dorsal horn. *Mol. Pain*. **7**, 76 (2011).

40. S. Y. X. Tiong, E. Polgár, J. C. van Kralingen, M. Watanabe, A. J. Todd, Galanin-immunoreactivity identifies a distinct population of inhibitory interneurons in laminae I-III of the rat spinal cord. *Mol. Pain*. **7**, 36 (2011).

41. S. S. Schattauer, J. R. Kuhar, A. Song, C. Chavkin, Nalfurafine is a G-protein biased agonist having significantly greater bias at the human than rodent form of the kappa opioid receptor. *Cell. Signal.* **32**, 59–65 (2017).

42. J. S. Lin, Y. Hou, K. Sakai, M. Jouvet, Histaminergic descending inputs to the mesopontine tegmentum and their role in the control of cortical activation and

wakefulness in the cat. *J. Neurosci.* **16**, 1523–1537 (1996).

43. M. Tashiro *et al.*, Dose dependency of brain histamine H(1) receptor occupancy following oral administration of cetirizine hydrochloride measured using PET with [11C]doxepin. *Hum. Psychopharmacol.* **24**, 540–548 (2009).

44. P. B. Reiner, A. Kamondi, Mechanisms of antihistamine-induced sedation in the human brain: H1 receptor activation reduces a background leakage potassium current. *Neuroscience*. **59**, 579–588 (1994).

45. M. M. Thakkar, Histamine in the regulation of wakefulness. *Sleep Med. Rev.* **15**, 65–74 (2011).

46. J. S. Anwari, S. Iqbal, Antihistamines and potentiation of opioid induced sedation and respiratory depression. *Anaesthesia*. **58**, 494–495 (2003).

47. M.-C. Ko, S. M. Husbands, Effects of atypical kappa-opioid receptor agonists on intrathecal morphine-induced itch and analgesia in primates. *J. Pharmacol. Exp. Ther.* **328**, 193–200 (2009).

48. H. Lee, N. N. Naughton, J. H. Woods, M.-C. Ko, Effects of butorphanol on morphine-induced itch and analgesia in primates. *Anesthesiology*. **107**, 478–485 (2007).

49. Y. Yamamoto *et al.*, Prediction of human CNS pharmacokinetics using a physiologically-based pharmacokinetic modeling approach. *Eur. J. Pharm. Sci.* **112**, 168–179 (2018).

50. G. W. Pasternak, Multiple opiate receptors: déjà vu all over again. *Neuropharmacology*. **47 Suppl 1**, 312–323 (2004).

51. T. Andoh *et al.*, Evidence for separate involvement of different mu-opioid receptor subtypes in itch and analgesia induced by supraspinal action of opioids. *J. Pharmacol. Sci.* **106**, 667–670 (2008).

52. A. T. Sia *et al.*, A118G single nucleotide polymorphism of human mu-opioid receptor gene influences pain perception and patient-controlled intravenous morphine consumption after intrathecal morphine for postcesarean analgesia. *Anesthesiology*. **109**, 520–526 (2008).

53. C. Kilkenny *et al.*, Animal research: reporting in vivo experiments: the ARRIVE guidelines. *Br. J. Pharmacol.* **160**, 1577–1579 (2010).

54. H. Ding *et al.*, Supraspinal actions of nociceptin/orphanin FQ, morphine and substance P in regulating pain and itch in non-human primates. *Br. J. Pharmacol.* **172**, 3302–3312 (2015).

55. M. C. Ko *et al.*, Intracisternal nor-binaltorphimine distinguishes central and peripheral kappa-opioid antinociception in rhesus monkeys. *J. Pharmacol. Exp. Ther.* **291**, 1113–1120 (1999).

56. K. Hargreaves, R. Dubner, F. Brown, C. Flores, J. Joris, A new and sensitive method for measuring thermal nociception in cutaneous hyperalgesia. *Pain*. **32**, 77–88 (1988).

57. T. Akiyama *et al.*, Mouse model of touch-evoked itch (alloknesis). *J. Invest. Dermatol.* **132**, 1886–1891 (2012).

58. J. Hachisuka *et al.*, Semi-intact ex vivo approach to investigate spinal somatosensory circuits. *elife*. **5** (2016), doi:10.7554/eLife.22866.

59. J. Hachisuka, H. R. Koerber, S. E. Ross, Selective-cold output through a distinct subset of lamina I spinoparabrachial neurons. *Pain*. **161**, 185–194 (2020).

60. P. Szucs, V. Pinto, B. V. Safronov, Advanced technique of infrared LED imaging of unstained cells and intracellular structures in isolated spinal cord, brainstem, ganglia and cerebellum. *J. Neurosci. Methods*. **177**, 369–380 (2009).

61. B. V. Safronov, V. Pinto, V. A. Derkach, High-resolution single-cell imaging for functional studies in the whole brain and spinal cord and thick tissue blocks using light-emitting diode illumination. *J. Neurosci. Methods*. **164**, 292–298 (2007).

Acknowledgments: We thank Dr. Jill Glausier and the Brain Tissue Donation Program at the University of Pittsburgh and the NIH NeuroBioBank for providing us with human spinal cord tissue. We thank Dr. Shiqun Zhang, Dr. Jamie Moy, and Dr. Michael S. Gold for scientific insight. We also thank Dr. Tayler Sheahan and Dr. Kelly Smith for editing the manuscript and Mr. Thomas Smith for his help with illustrations. Images were created with BioRender.com; **Funding:** Research reported in this publication was supported by the Virginia Kaufman Endowment Fund, NIH/NIAMS grant AR063772, NIH/NINDS grant NS096705 (S.E.R.), NIH/NIAMS grant AR069861 (M.C.K.), NRSA F31 grant F31NS113371 and NIGM/NIH T32GM008208 (E.N.); **Author contributions:** E.N. performed mouse stereotaxic injections, behavior, and analysis. J.H. conducted slice electrophysiology experiments. E.N. performed anatomical and histological analyses of mouse and human spinal cords. E.N. and G.L. obtained and analyzed patient data. H.D. and M.C.K. performed experiments in non-human primates. E.N. and S.E.R. conceived experiments, interpreted data and wrote the manuscript. All authors edited the manuscript; **Competing interests:** Authors declare no competing interests; and **Data and materials availability:** All data associated with this study are in the paper or supplementary materials. Mcpt5$_{Cre}$ mice were a gift from Axel Roers (Dresden University of Technology) and fresh human spinal cord tissues were provided by the NIH NeuroBioBank.

Figures:

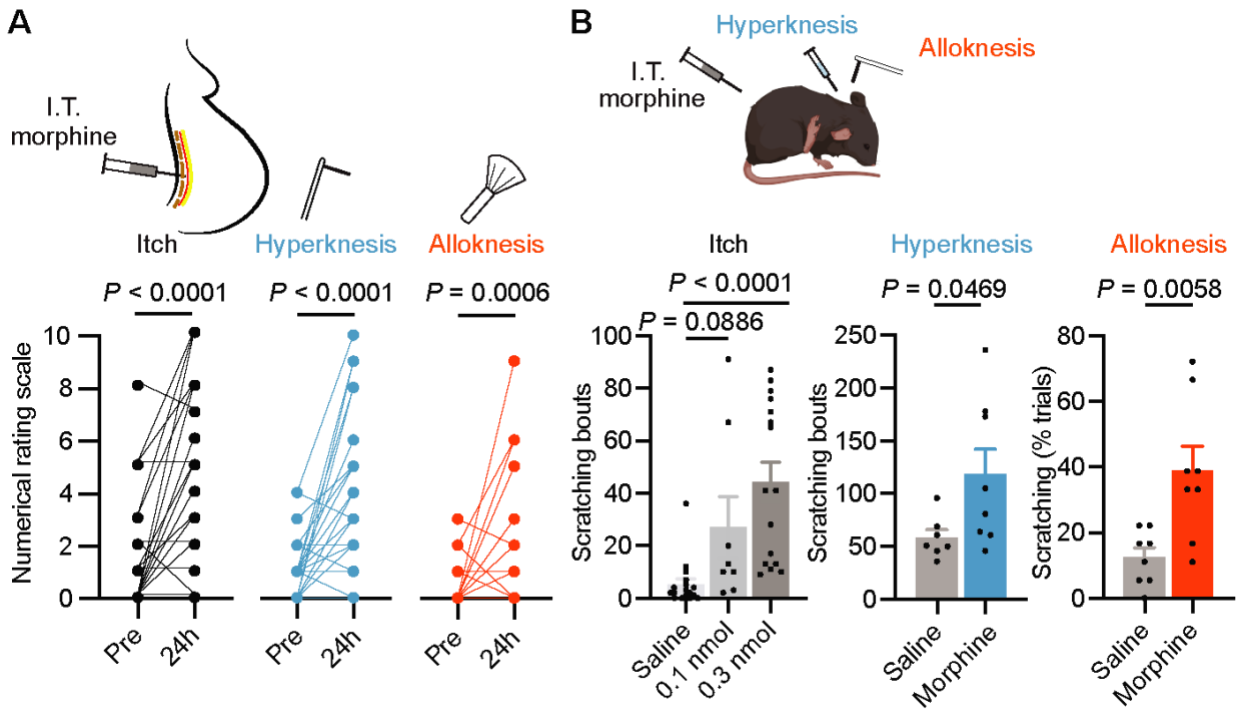

Fig 1. Endpoints for sensitization caused by morphine-induced itch in human subjects and in mice.

(A) I.T. morphine-induced itch, hyperknesis, and alloknesis in obstetric patients. I.T., intrathecal. *n* = 39 human subjects. (**B)** I.T. morphine-induced itch, hyperknesis, and alloknesis in mice. *n* = 7-9 mice per group. *P* values were determined by (A) Wilcoxon matched-pairs signed rank test and (B) one-way ANOVA, with Bonferroni's correction and two-tailed unpaired t-test. (A) data points represent individual human subjects pre and post spinal morphine (B) and data are mean + S.E.M with dots representing individual mice.

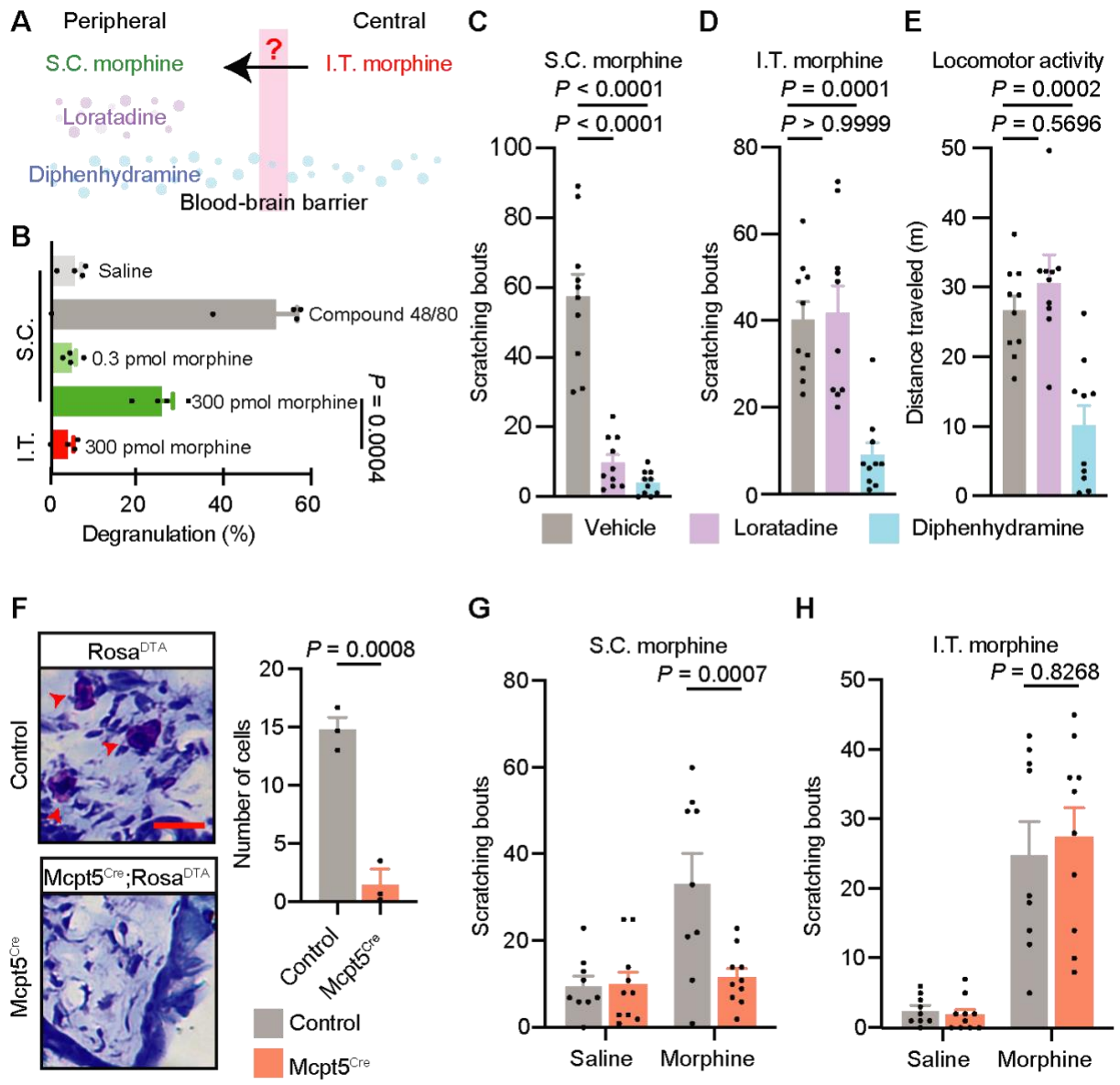

Fig 2. Intrathecal morphine-induced itch is mast-cell independent

(A) Schematic describing the pharmacological strategy to determine how morphine causes itch. I.T., intrathecal and S.C., subcutaneous. **(B)** Quantification of degranulated mast cells. *n* = 4 mice per group. **(C** to **E)** Effect of antihistamines on **(C)** S.C. morphine-induced itch **(D)** I.T. morphine-induced itch, **(E)** and locomotor activity. *n* = 10 mice per group. **(F)** Mast cell deletion and quantification in Mcpt5^{Cre}; Rosa^{DTA} mice. *n* = 3 mice per group. Scale bar = 10 μm. **(G)** Effect of mast cell depletion on **(G)** S.C. morphine-induced itch **(H)** and I.T. morphine-induced itch. *n* = 9-10 mice per group. *P* values were determined by (B to E) one-way ANOVA, with Bonferroni's correction, (F) two-tailed, unpaired t-test, (G and H) and two-way ANOVA with Bonferroni's correction. (B to H) data are mean + S.E.M with dots representing individual mice.

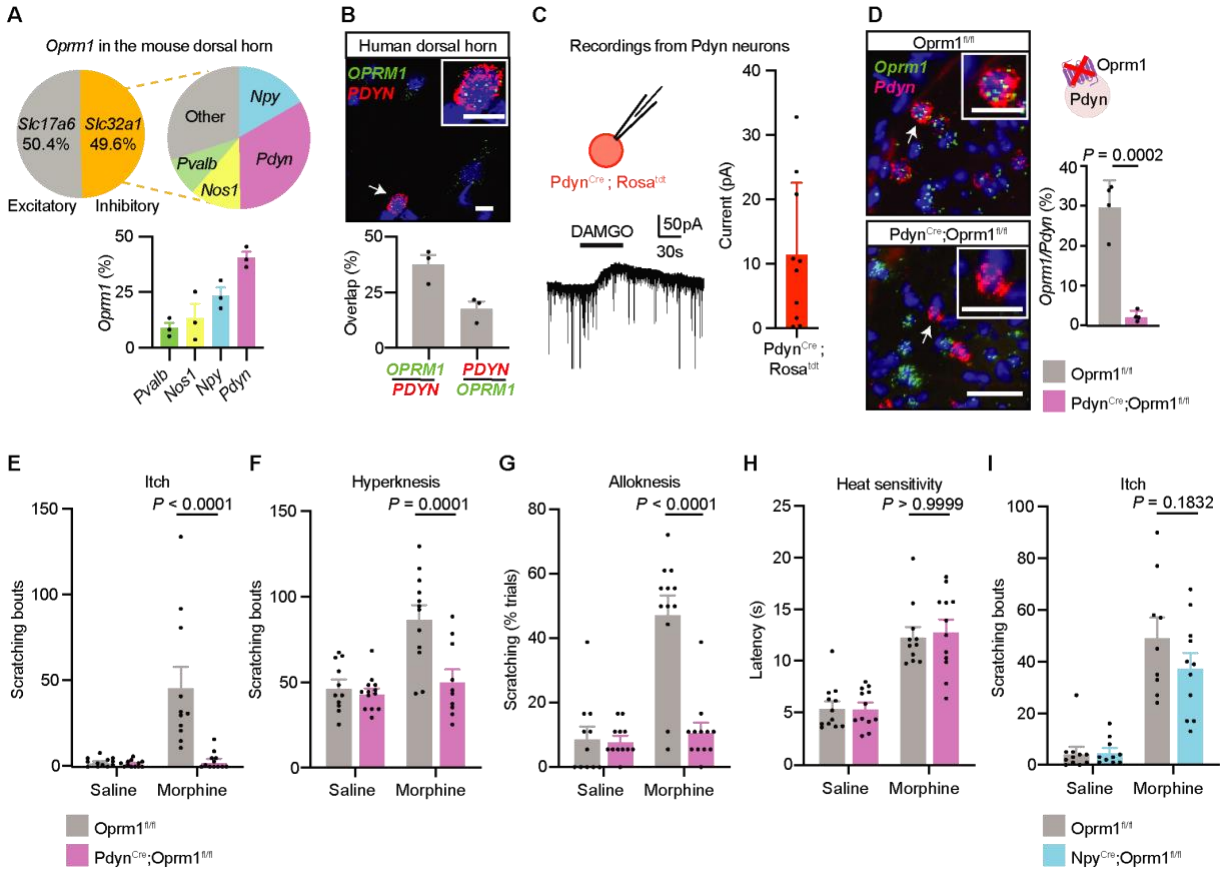

Fig. 3. *Oprm1* expression in Pdyn neurons is required for morphine-induced itch.

(A) *Oprm1* expression in neurons in the mouse spinal dorsal horn. *n* = 3 mice. **(B)** Fluorescent in-situ hybridization of human spinal dorsal horn depicting the co-expression of *OPRM1* and *PDYN*. *n* = 3 individual dorsal horns. Arrow indicates the cell shown in the inset. Scale bar = 50 µm. **(C)** Electrophysiological recordings of $Pdyn^{Cre}$; $Rosa^{tdt}$ neurons in the presence of DAMGO. *n* = 10 neurons. **(D)** Deletion of *Oprm1* in *Pdyn* neurons in the spinal dorsal horn of $Pdyn^{Cre}$; $Oprm1^{fl/fl}$ animals compared to $Oprm1^{fl/fl}$ controls. Arrow indicates the cell shown in the inset. Scale bar = 50 µm, inset = 25 µm. *n* = 4 mice per group. **(E** to **G)** Effect of deletion of *Oprm1* in Pdyn neurons on morphine-induced **(E)** itch **(F)** hyperknesis, **(G)** alloknesis, **(H)** and heat sensitivity. *n* = 11-13 mice per group. **(I)** Effect of *Oprm1* deletion in Npy neurons on morphine-induced itch. *n* = 12 mice per group. *P* values were determined by (D) two-tailed, unpaired t-test., (E to I), two-way ANOVA, with Bonferroni's correction. (A to I) Data are mean + S.E.M. with individual dots representing (A and D to I) individual mice, (B) individual human dorsal horns, (C) and individual neurons.

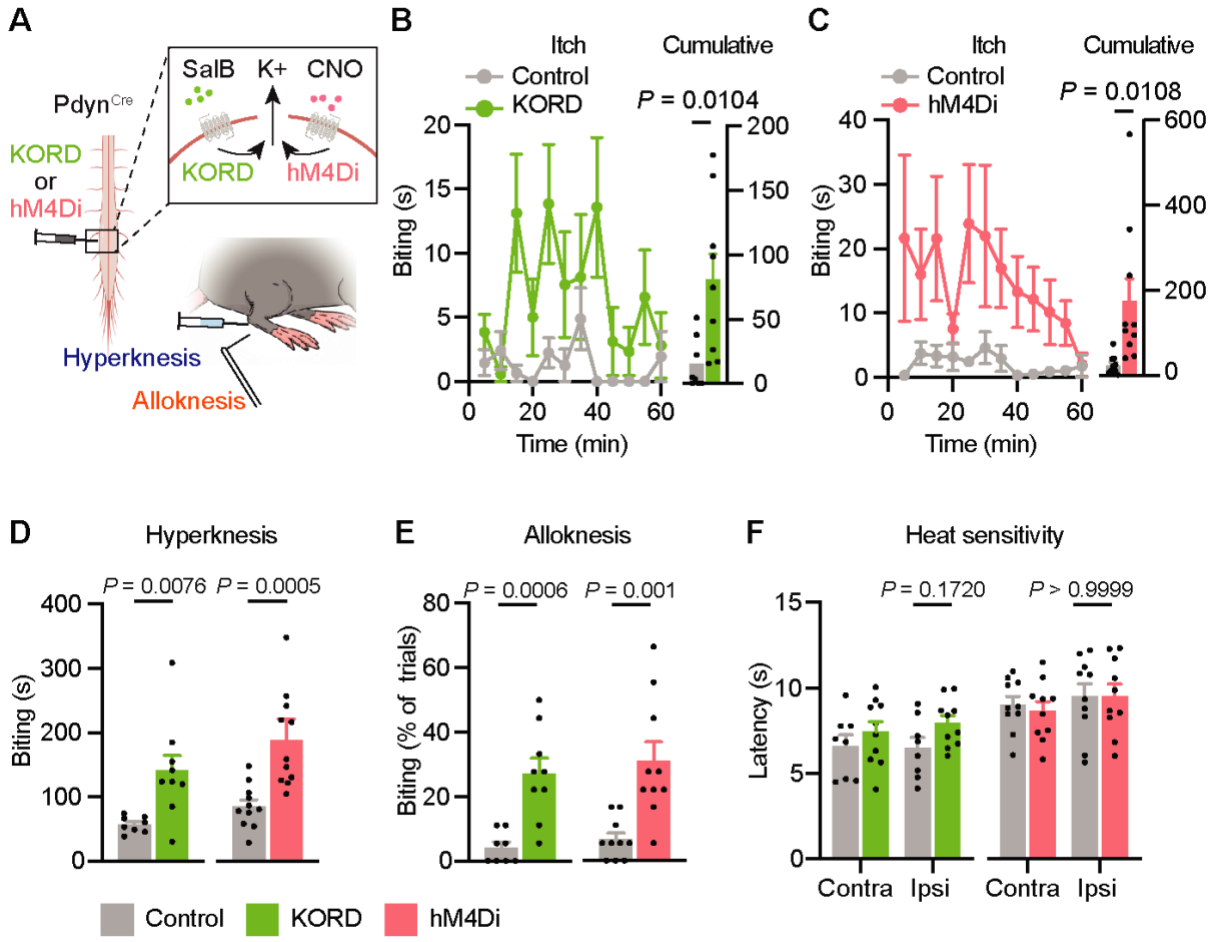

Fig. 4. Inhibition of Pdyn neurons is sufficient to evoke itch

(A) Experimental design. **(B** and **C)** Time course of itch following chemogenetic inhibition of Pdyn neurons with **(B)** KORD **(C)** or hM4Di. **(D** to **F)** Chemogenetic inhibition of Pdyn neurons with KORD (green, left) and hM4Di (pink, right) on **(D)** hyperknesis, **(E)**, alloknesis, **(F)** and heat sensitivity. *n* = 7-11 mice per group. *P* values were determined by (B to E) two-tailed, unpaired t-test (F) and two-way ANOVA, with Bonferroni's correction. (B, C) Time course data are mean ± S.E.M. (B to F) data are mean + S.E.M. with individual dots representing individual mice.

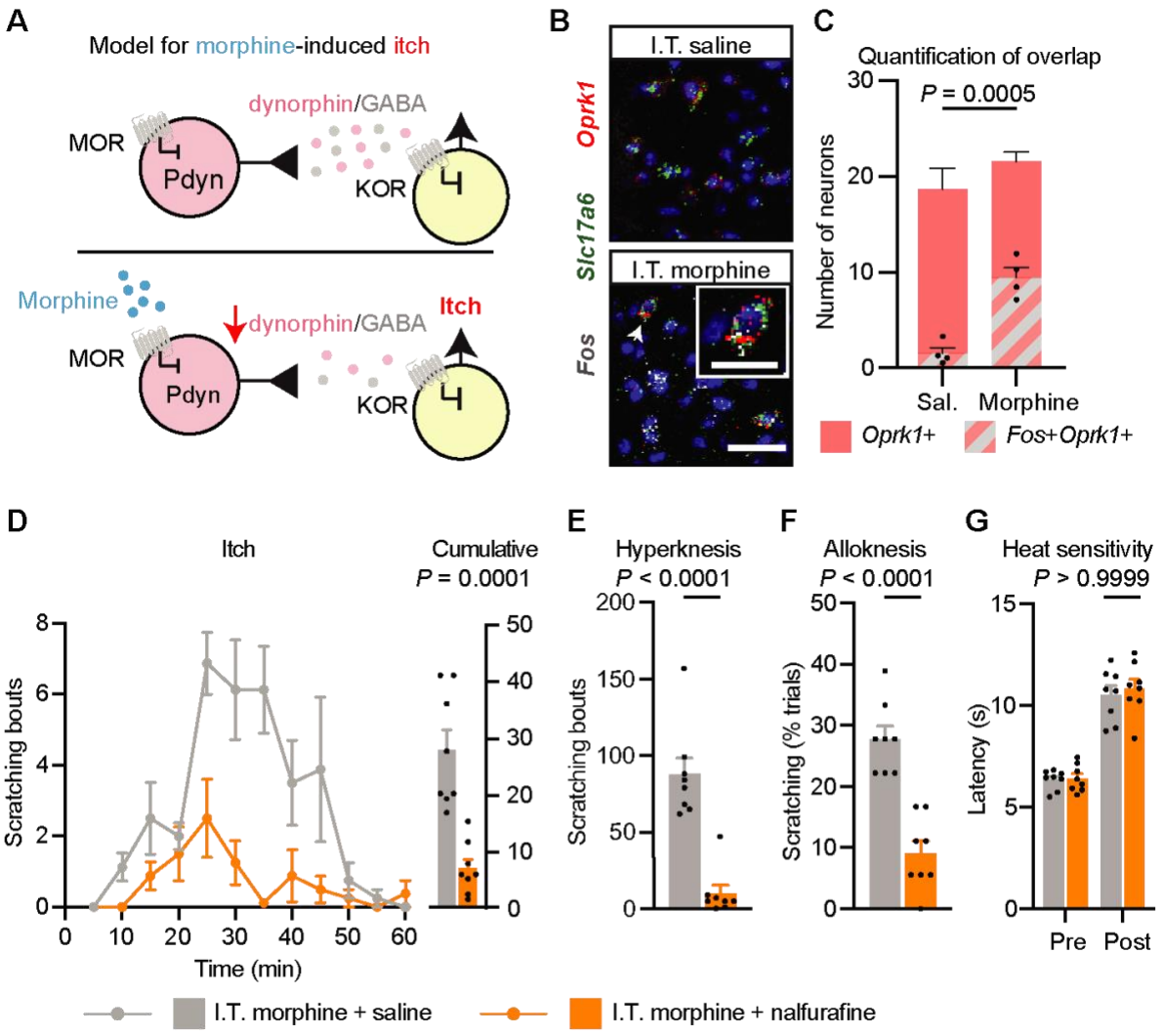

Fig. 5. Oprk1 signaling alleviates morphine-induced itch in mice.

(A) Model for morphine-induced itch. **(B)** Representative image for the expression of *Fos* in excitatory (*Slc17a6* containing) *Oprk1* neurons. Arrow indicates the cell shown in the inset. Scale bar = 50 μm, inset = 25 μm. **(C)** Quantification of B. *n* = 3 mice. **(D** to **G)**, in mice, the effect of nalfurafine (40 ng) on morphine-induced **(D)** itch, **(E)** hyperknesis, **(F)** alloknesis, **(G)** and heat sensitivity. *n* = 8 mice per group. *P* values were determined by (D to F) two-tailed, unpaired t-test and (G) two-way ANOVA, with Bonferroni's correction. (C to G) Data are mean + S.E.M. with dots representing individual mice. (D) Time course data are mean ± S.E.M.

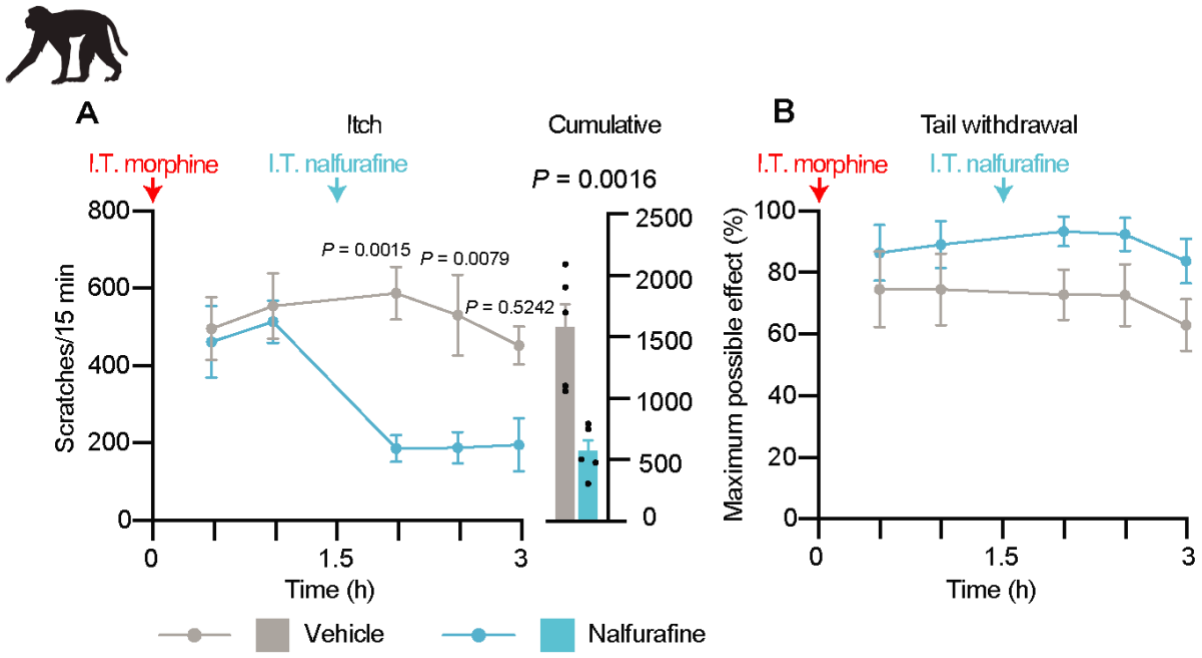

Fig. 6. I.T. nalfurafine alleviates morphine-induced itch in non-human primates.

(A) The effect of nalfurafine (10 μg) on I.T. morphine-induced itch. *P* values were determined by two-way ANOVA, with Bonferroni's correction (left) and two-tailed, unpaired t-test (right). **(B)** Effect of nalfurafine (10 μg) on tail-withdrawal. $n = 5$ primates per group. No significant effect was found between saline and nalfurafine using a two-way ANOVA ($P = .8924$). Data are mean + S.E.M. with dots representing individual primates. Time course data are mean ± S.E.M.

Supplementary Materials for

Morphine causes itch through a distinct disinhibitory circuit

Eileen Nguyen, Grace Lim, Huiping Ding, Junichi Hachisuka, Mei-Chuan Ko, and Sarah E. Ross*

*Corresponding author. Email: saross@pitt.edu

This PDF file includes:

Fig. S1. Morphine-induced itch, hyperknesis, and alloknesis in obstetric patients.
Fig. S2. Morphine-induced itch, hyperknesis, and alloknesis in mice.
Fig. S3. Differential role of mast cells on subcutaneous vs. intrathecal morphine-induced itch.
Fig. S4. Spinal expression of *Oprm1* in *Grpr*, *Pdyn*, and *Npy* neurons.
Fig. S5. Expression of *Oprm1* in *Npy* neurons is not required for morphine-induced itch
Fig. S6. Validation of viral infection of Pdyn neurons.
Fig. S7. Dose-response analysis of nalfurafine treatment for morphine-induced itch.
Fig. S8. Antagonism of the kappa-opioid receptor evokes itch.

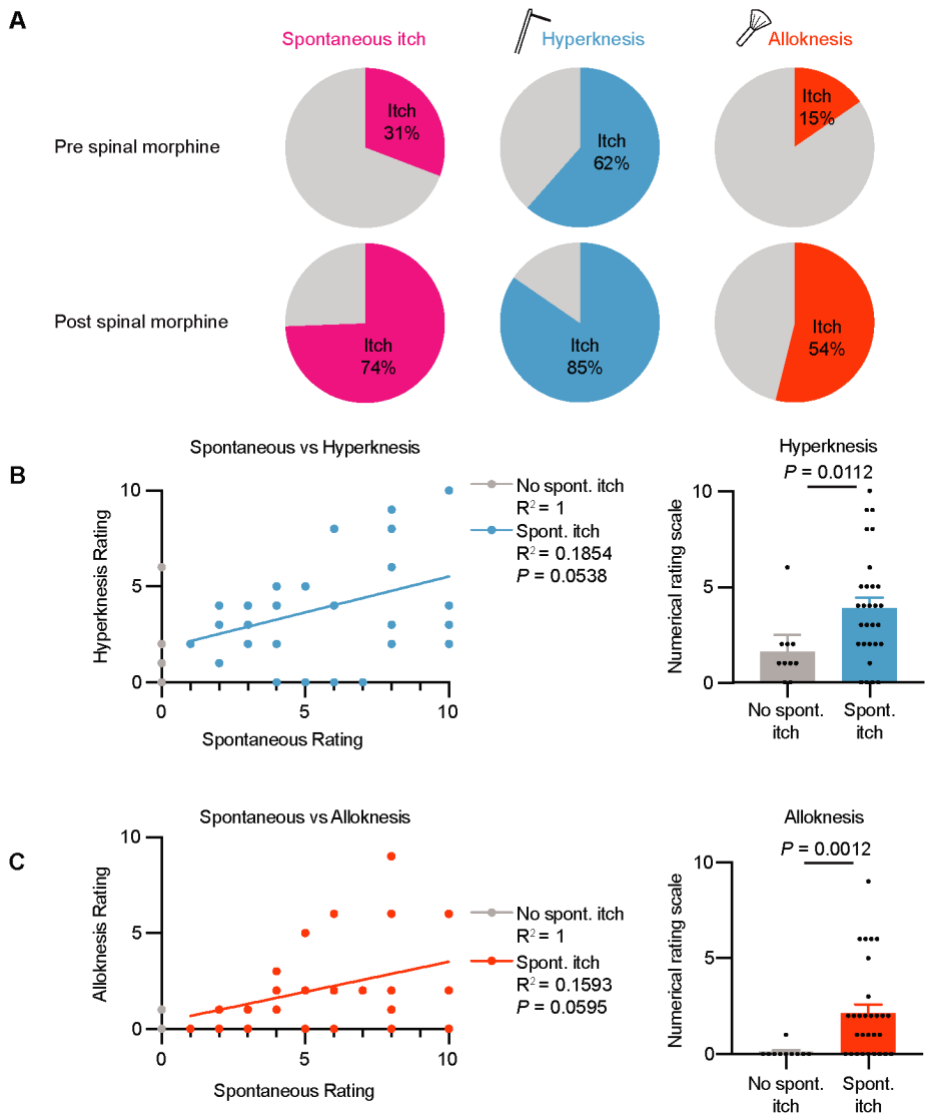

Fig. S1. Morphine-induced itch, hyperknesis, and alloknesis in obstetric patients.

(A) Proportion of women reporting itch, hyperknesis, and alloknesis before and after spinal morphine. **(B** and **C)** Correlation between subjects' spontaneous score and **(B)** hyperknesis score **(C)** and alloknesis score. *n* = 39 subjects. (B and C) *P* values were determined by a linear regression (left) and Mann-Whitney test (right). Data are mean + S.E.M with dots representing individual patients.

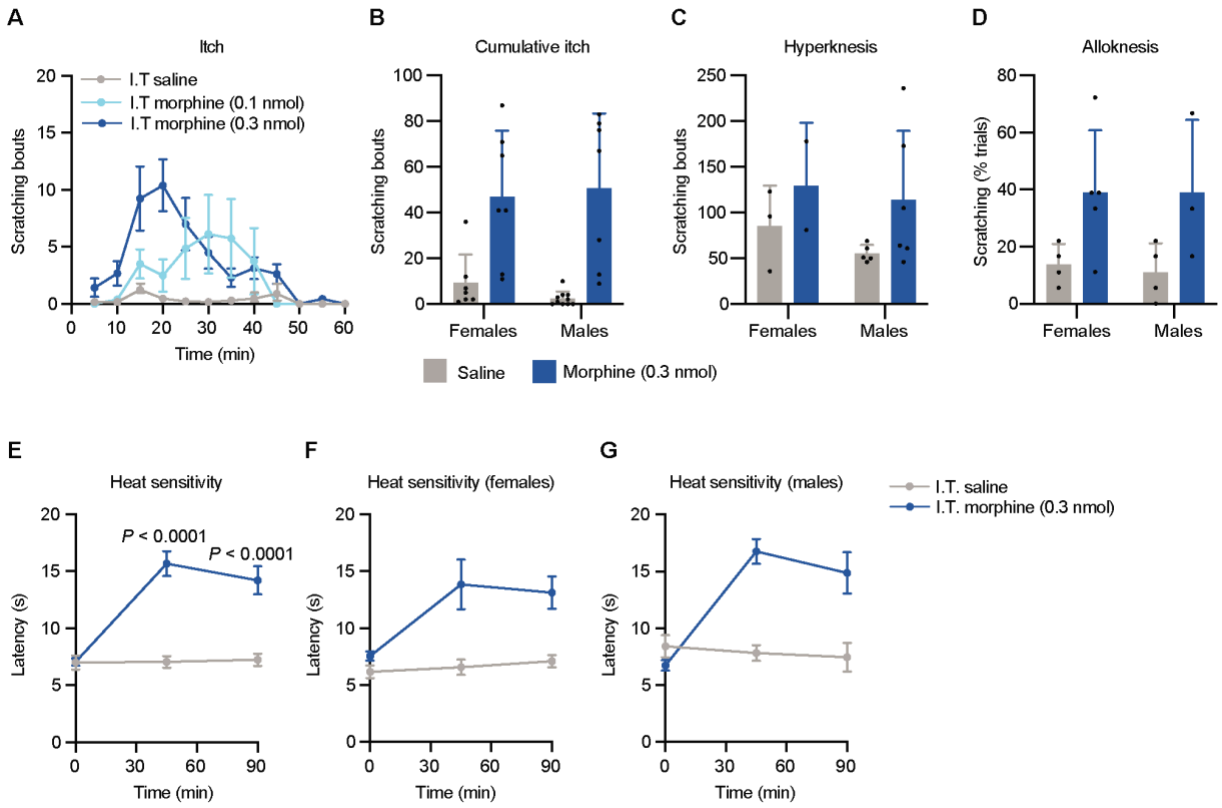

Fig. S2. Morphine-induced itch, hyperknesis, and alloknesis in mice.

(A) Time course of itch following I.T. administration of morphine (100 pmol and 300 pmol) and saline. *n* = 7-9 mice per group. **(B** to **D)** Effect of morphine-induced **(B)** itch, **(C)** hyperknesis, **(D)** and alloknesis separated by sex. *n* = 3-4 mice per group. **(E)** Effect of I.T. morphine on heat sensitivity. *n* = 7-9 mice per group, two-way ANOVA with Bonferroni's correction. **(F** and **G)** Effect of morphine on heat sensitivity among **(F)** female **(G)** and male mice. (A and E to G) Data are mean ± S.E.M. (B to D) Data are mean + S.E.M. with individual dots representing individual mice.

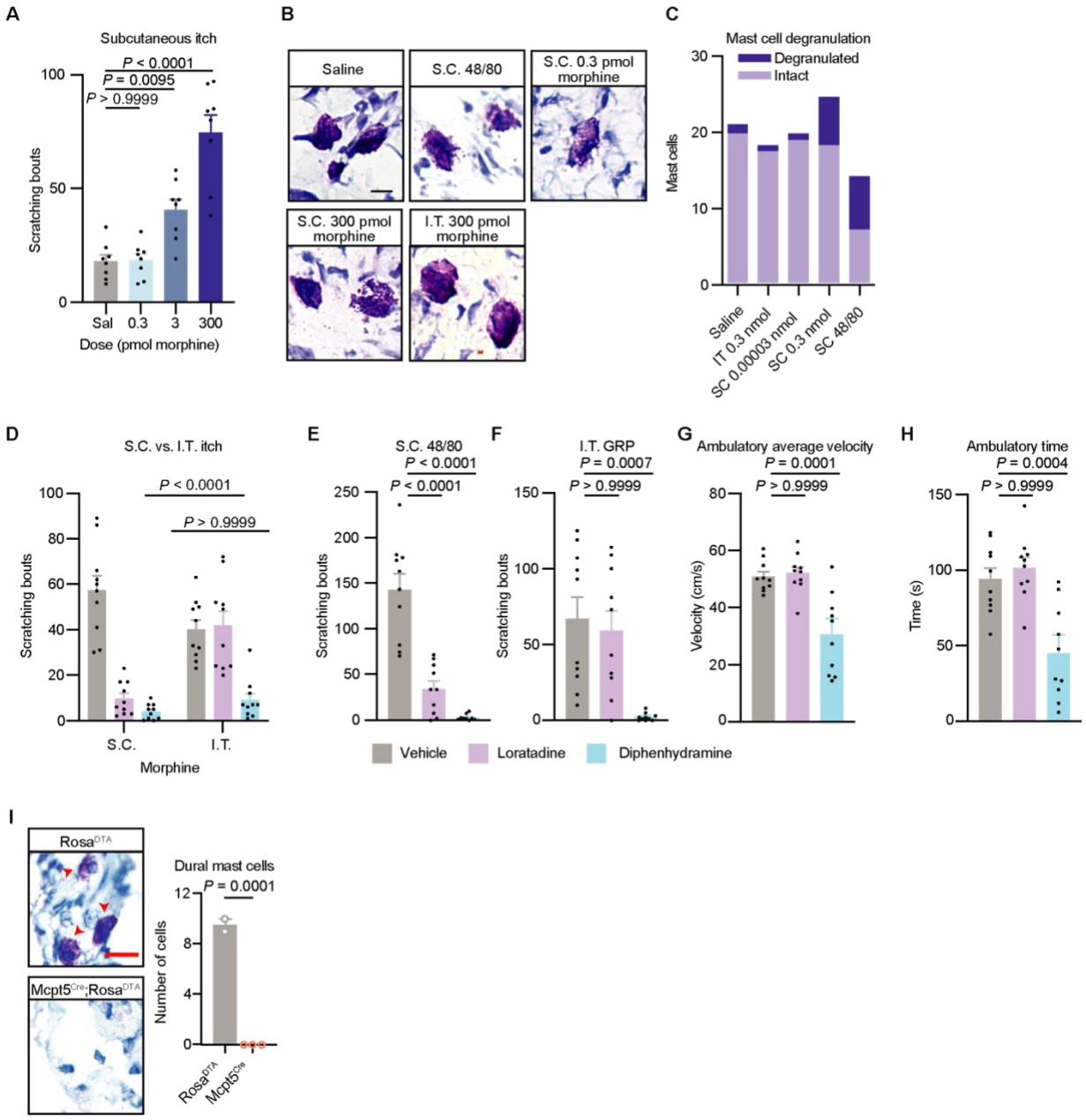

Fig. S3. Differential role of mast cells on subcutaneous vs. intrathecal morphine-induced itch.

(A) Itch caused by escalating doses of S.C. morphine. *n* = 8 mice per group. **(B)** Representative images of cutaneous mast cells. Scale bar = 10 μm. **(C)** Quantification of B**.** *n* = 4 mice per group. **(D** to **H)** Comparison of the effects of antihistamines on **(D)** S.C. and I.T. morphine-induced itch, **(E)** S.C. 48/80 induced itch, **(F)** I.T. GRP induced itch, **(G)** ambulatory velocity, **(H)** and ambulatory time. (D to H) *n* = 10 mice per group. (**I)** Validation of dural mast cell deletion in Mcpt5$_{Cre}$; Rosa$_{DTA}$ mice. *n* = 2-3 mice per group. *P* values were determined by (A and E to H) one-way ANOVA, with Bonferroni's correction, (D) two-way ANOVA, with Bonferroni's correction (I) and two-tailed, unpaired t-test. (A and D to I) Data are mean + S.E.M with dots representing individual mice.

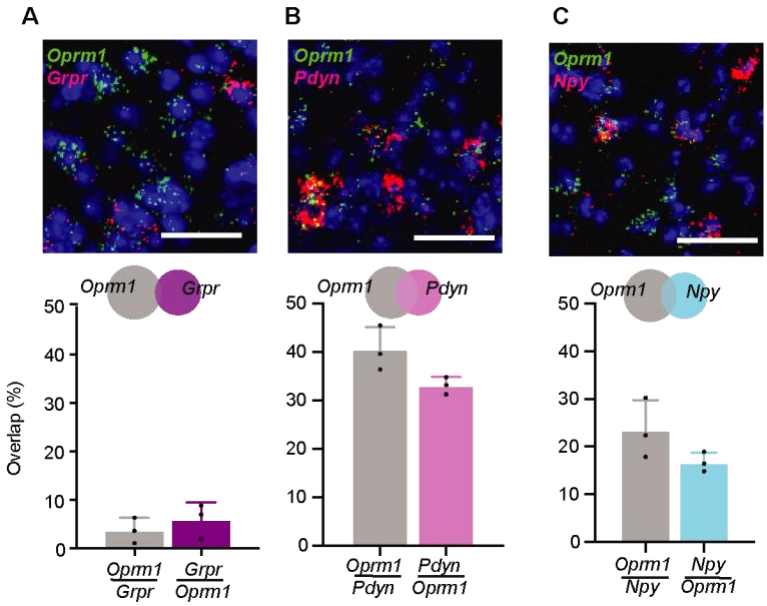

Fig. S4. Spinal expression of *Oprm1* in *Grpr*, *Pdyn*, and *Npy* neurons.

(A to **C)** Representative image of fluorescent in-situ hybridization in the spinal dorsal horn comparing expression of *Oprm1* to **(A)** *Grpr*, **(B)** *Pdyn*, **(C)** and *Npy*. The overlap is quantified below. Scale bar = 50 μm. *n* = 3 mice. Data are mean + S.E.M with dots representing individual mice.

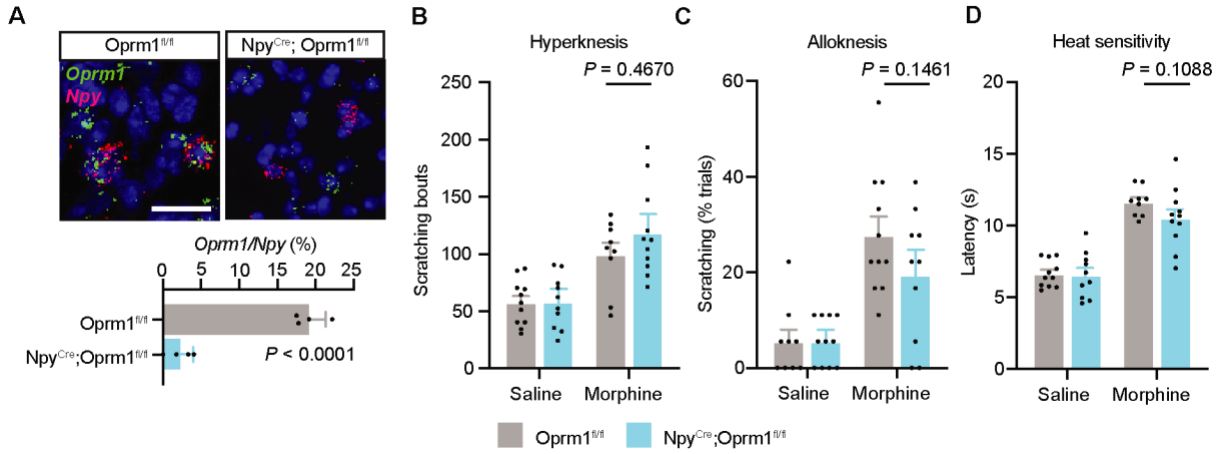

Fig. S5. Expression of *Oprm1* in *Npy* neurons is not required for morphine-induced itch

(A) Fluorescent in-situ hybridization to validate deletion of *Oprm1* in *Npy* neurons in the spinal dorsal horn in Npy$_{Cre}$; Oprm1$_{fl/fl}$ animals compared to Oprm1$_{fl/fl}$ controls. Scale bar = 50 µm. *n* = 4 mice per group. **(B** to **D)** Deletion of Oprm1 in Npy neurons on morphine-induced **(B)** hyperknesis, **(C)** alloknesis, **(D)** and heat sensitivity. *n* = 12 mice. *P* values were determined by (A) two-tailed, unpaired t-test, (B to D) and two-way ANOVA, with Bonferroni's correction. Data are mean + S.E.M with dots representing individual mice.

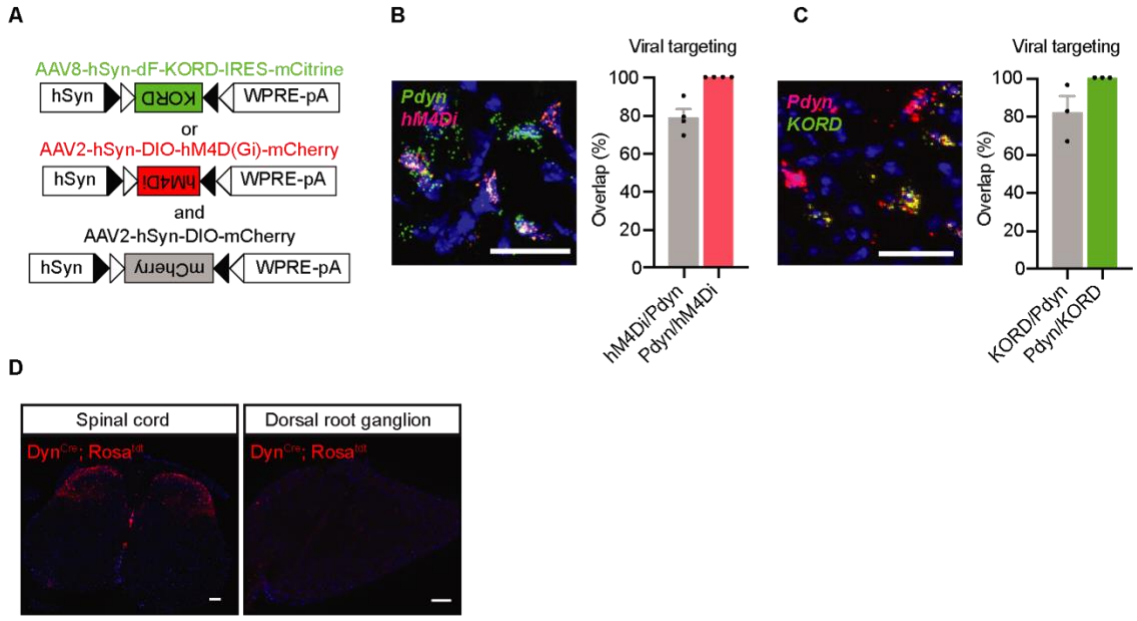

Fig. S6. Validation of viral infection of Pdyn neurons.

(A) Cre-dependent viruses used to selectively express KORD and hM4Di DREADDs into the spinal cord of Pdyn$_{Cre}$ mice. **(B** and **C)** Representative image of fluorescent in-situ hybridization (left) and quantification (right) of the dorsal horn in Pdyn$_{Cre}$ mice injected with **(B)** hM4Di **(C)** and KORD. *n* = 3 mice per group. **(D)** Representative image of a spinal cord and dorsal root ganglion section in Pdyn$_{Cre}$; Rosa$_{tdt}$ mouse. Scale bar = 50 μm. (B and C) Data are mean + S.E.M with dots representing individual mice.

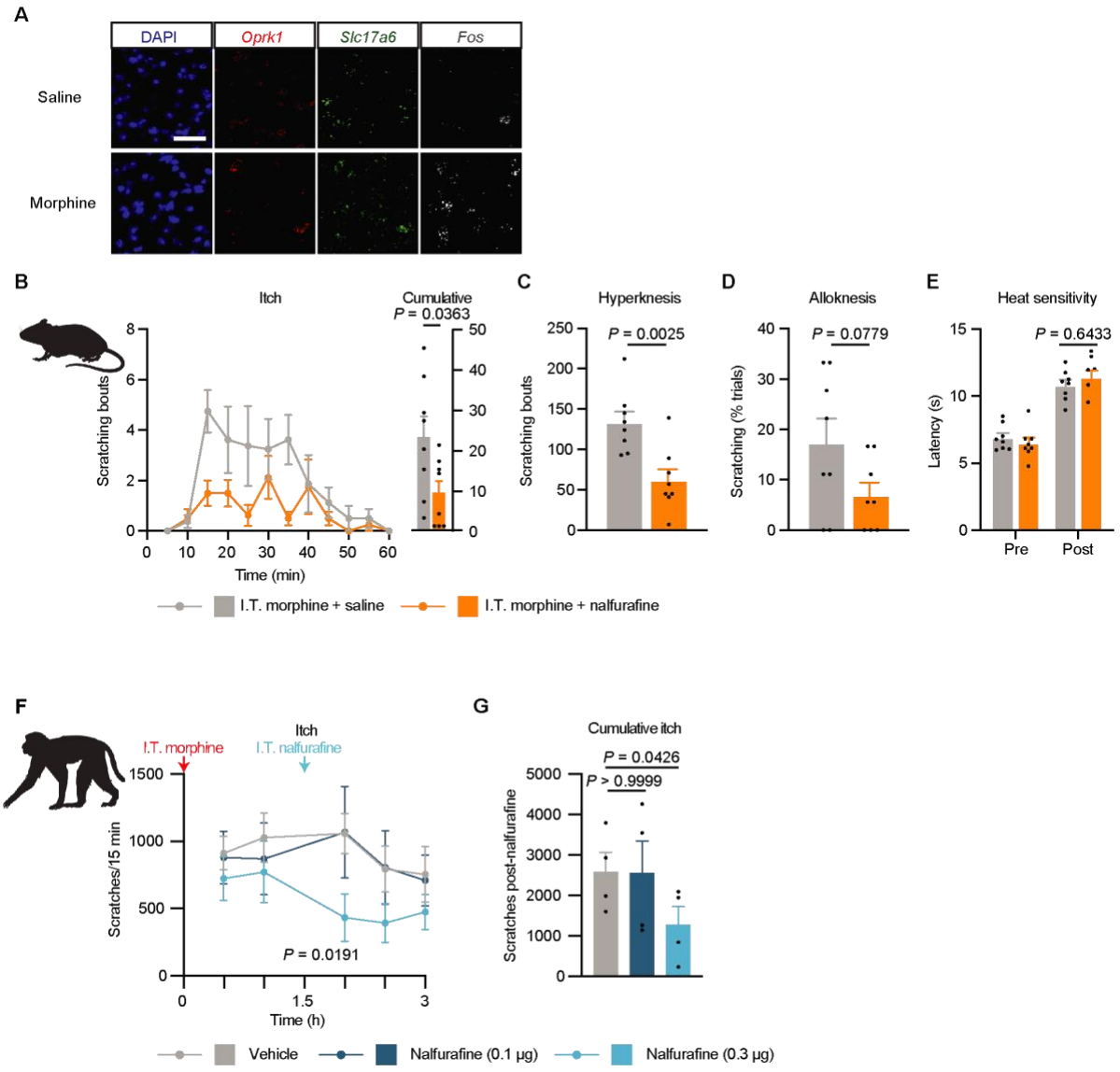

Fig. S7. Dose-response analysis of nalfurafine treatment for morphine-induced itch.

(A) Representative image for the expression of *Fos* in *Oprk1* neurons containing *Slc17a6*. These panels are shown merged in the main figure. Scale bar = 50 µm. **(B** to **E)** in mice, the effect of nalfurafine (1.25 ng) on morphine-induced **(B)** itch, **(C)** hyperknesis, **(D)** alloknesis, **(E)** and heat sensitivity. *n* = 8 mice per group. **(F** and **G)** in primates, the effect of nalfurafine (10 ug) following I.T. morphine (30 ug) on itch **(F)** as a time course, **(G)** and cumulatively over 60 minutes. *n* = 4 primates per group. *P* values were determined by (B to D) two-tailed, unpaired t-test, (E and F) two-way ANOVA, with Bonferroni's correction, (G) and one-way ANOVA with Bonferroni's correction. (B and F) Time course data are mean ± S.E.M. (B to E and G) data are mean + S.E.M with dots representing individual (B to E) mice, (G) and primates.

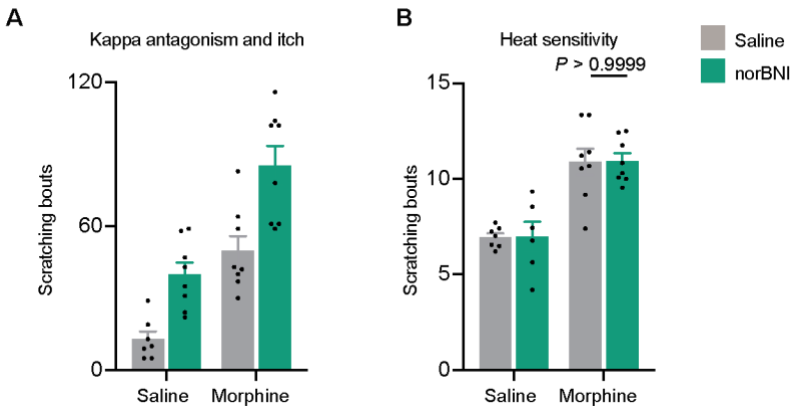

Fig. S8. Antagonism of the kappa-opioid receptor evokes itch

(A) Antagonism of the kappa-opioid receptor with nor-Binaltorphimine dihydrochloride (norBNI) on spontaneous and morphine-induced itch. A significant main effect of norBNI was observed ($P < 0.0001$) and morphine ($P < 0.0001$), but the interaction was not significant ($P = .4876$). *P* values were determined by two-way ANOVA. **(B)** Oprk1 antagonism on morphine-induced analgesia to heat sensitivity. $n = 6$-8 mice per group. *P* value was determined by two-way ANOVA with Bonferroni's correction. Data are mean + S.E.M with dots representing individual mice.